WEIGHTING MATRIX SELECTION FOR QFT DESIGNS

THESIS

George R. Rivard
Captain, USAF

AFIT/GE/ENG/89D-43

DEPARTMENT OF THE AIR FORCE
AIR UNIVERSITY
AIR FORCE INSTITUTE OF TECHNOLOGY

Wright-Patterson Air Force Base, Ohio

AFIT/GE/ENG/89D-43

WEIGHTING MATRIX SELECTION FOR QFT DESIGNS

THESIS

Presented to the Faculty of the School of Engineering
of the Air Force Institute of Technology
Air University
In Partial Fulfillment of the
Requirements for the Degree of
Master of Science in Electrical Engineering

George R. Rivard, B.S.E.E., M.S.E.M.
Captain, USAF

December, 1989

Preface

The use of the Quantitative Feedback Technique (QFT) in determining designs that satisfy performance criteria for a set of plants having structured parameter uncertainties rests heavily on the invertibility of the plant matrix. While other design constraints are appropriate, it is the requirement for plant invertability that forces the designer to either square-down or square-up a nonsquare plant matrix. This study investigates the use of a frequency sensitive weighting matrix in squaring-down a nonsquare plant having more inputs that outputs.

The research portions of this study concentrate in three primary areas: linear algebra, H_2 and H_∞-norm minimization, and QFT control theory. Without the help and understanding of experts in each of these areas, it is doubtful that I would have completed this thesis. As such, I would like to express my gratitude to Professor Katri, Captain Ridgely, and Professor Houpis.

In addition, I would like to thank my advisor Lt Col Lewantowicz. His knowledge, research experience, and periodic pep-talks were essential to the completion of this thesis despite the difficulties that were encountered.

Finally, I would like to thank my wife Ingrid and daughter Doris for enduring the sleepless nights and curtailed levels of patience that accompanied this thesis effort.

George R. Rivard

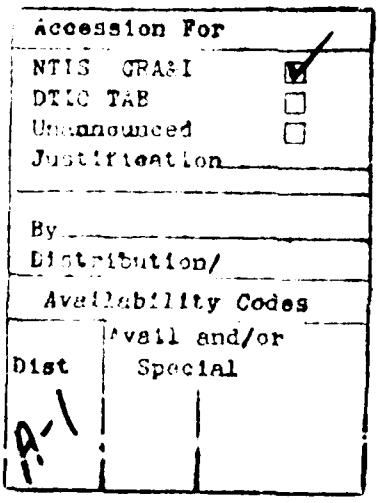

Table of Contents

List of Figures

List of Tables

Symbols

$\mathbf{B}(\mathrm{j}\omega)$	$\equiv$	$\mathbf{P_e^{-1}}(\mathrm{j}\omega) - \mathbf{D}(\mathrm{j}\omega)$.
BNIC	$\equiv$	basically noninteracting.
$\mathbf{d_i}(\mathrm{j}\omega)$	$\equiv$	QFT plant disturbance models.
$\mathbf{D}(\mathrm{j}\omega)$	$\equiv$	diagonal elements of $\mathbf{P_e^{-1}}(\mathrm{j}\omega)$.
det	$\equiv$	determinant of a matrix.
E	$\equiv$	energy.
f_{ij}	$\equiv$	element ij of $\mathbf{F}(\mathrm{j}\omega)$.
$\mathbf{F}(\mathrm{j}\omega)$	$\equiv$	Fourier transform of QFT determined input filter, or prefilter.
g_{ij}	$\equiv$	element ij of $\mathbf{G}(\mathrm{j}\omega)$.
$\mathbf{G}(\mathrm{j}\omega)$	$\equiv$	Fourier transform of QFT determined cascade compensator.
H_2, H_∞	$\equiv$	2-norm and ∞-norm Hardy spaces.
inf	$\equiv$	infimum.
LHP	$\equiv$	left half plane.
LTI	$\equiv$	linear time invariant.
m_{ij}	$\equiv$	element of P_e^{-1}.
MIMO	$\equiv$	multiple-input multiple-output.
MISO	$\equiv$	multiple-input single-output.
MP	$\equiv$	minimum-phase.
NMP	$\equiv$	nonminimum-phase.
p	$\equiv$	aircraft roll rate.
p_{ij}	$\equiv$	element ij of $\mathbf{P}(\mathrm{j}\omega)$.
$p_{e_{ij}}$	$\equiv$	element ij of P_e.
$\overline{p_{ij}}$	$\equiv$	complex congugate of element ij of P.
$p(t)$	$\equiv$	time domain signal or SISO plant.
P	$\equiv$	indicates either $P(t)$ or $\mathbf{P}(\mathrm{j}\omega)$ is in use.

P_i	$\equiv$	squared-down version of $\mathbf{P}(\mathrm{j}\omega)$.
$P(t)$	$\equiv$	time domain uncompensated MIMO plant matrix.
$\mathbf{P}(\mathrm{j}\omega)$	$\equiv$	Fourier transform of MIMO plant matrix.
$\mathcal{P}(\mathrm{j}\omega)$	$\equiv$	Fourier transform of set of possible plant matrices
$\mathbf{P_e}(\mathrm{j}\omega)$	$\equiv$	Fourier transform of desired or equivalent plant matrix.
$\mathcal{P}_\mathbf{e}(\mathrm{j}\omega)$	$\equiv$	Fourier transform of desired set of possible plant matrices
q	$\equiv$	aircraft pitch rate.
q_{ij}	$\equiv$	element ij of $\mathbf{Q}(\mathrm{j}\omega)$.
Q_i	$\equiv$	squared-down version of $\mathbf{Q}(\mathrm{j}\omega)$.
$\mathbf{Q}(\mathrm{j}\omega)$	$\equiv$	Fourier transform of squaring-down compensator.
QFT	$\equiv$	Quantitative Feedback Technique.
r	$\equiv$	aircraft yaw rate.
$\mathbf{r}(\mathrm{j}\omega)$	$\equiv$	Fourier transform of aircraft command control input.
Re	$\equiv$	real part of.
RHP	$\equiv$	right half plane.
RH_∞	$\equiv$	subspace of H_∞ consisting of real rational functions in H_∞.
SISO	$\equiv$	single-input single-output.
sup	$\equiv$	supremum value.
$(.)^T$	$\equiv$	transpose of a matrix.
$\mathbf{T}(\mathrm{j}\omega)$	$\equiv$	control ratio used in developing MISO equivalent plant.
$\mathbf{T_i}(\mathrm{j}\omega)$	$\equiv$	fixed matrices of model-matching problem, $i \in (1,2,3)$.
$\mathbf{u}(\mathrm{j}\omega)$	$\equiv$	Fourier transform of control surface command input.
$\mathbf{u_{ij}}(\mathrm{j}\omega)$	$\equiv$	element ij of $\mathbf{U}(\mathrm{j}\omega)$.
$\mathbf{U}(\mathrm{j}\omega)$	$\equiv$	premultiplier matrix of a singular value decomposition.
W_i	$\equiv$	weighting matrix.
v_{ij}	$\equiv$	element of V matrix.

Abstract

This thesis investigates the selection of the frequency sensitive weighting matrix needed to convert a nonsquare $l \times m$ plant matrix into a square plant matrix that satisfies Quantitative Feedback Technique (QFT) multiple-input, multiple-output design constraints. The method of pre-specifying a desirable square plant matrix is used in determining the necessary weighting matrix. This study assumes that the nonsquare plant matrix has more inputs than outputs and the option to square-up is not available (i.e., it is assumed that inaccessible states cannot be reconstructed due to design limitations).

The thesis examines several topics. The topics include energy and power spectral densities, singular value decompositions of matrices of transfer functions, QFT design constraints, QFT designs accomplished on nonsquare plants by breaking up the nonsquare plant into a sum of square plants, and both H_2 and H_∞-norm minimization.

While it was desired to pursue this study effort through a complete QFT design, problems encountered in obtaining the frequency sensitive weighting matrices needed to satisfy a pre-determined desirable plant matrix made this impossible in the time available. As such, neither the optimal squaring-down compensators nor a final QFT design is presented.

This study concludes with an examination of problems encountered and recommendations for areas of future study that avoid the described problems.

WEIGHTING MATRIX SELECTION FOR QFT DESIGNS

I. Introduction

This thesis focuses on the selection of a frequency sensitive weighting matrix $\mathbf{Q}(j\omega)$ that converts an original non-square $l \times m$ plant transfer matrix $\mathbf{P}(j\omega)$ into a square plant matrix appropriate for a multiple-input, multiple-output (MIMO) quantitative feedback technique (QFT) design. The plant is assumed to have m control inputs and l outputs; the number of inputs is further assumed to exceed the number of outputs (i.e. states) available for feedback. The method of pre-specifying an $l \times l$ desirable plant transfer matrix $\mathbf{P_e}(j\omega)$ whose determinant is minimum-phase (MP) is used in determining the necessary nonsquare, $m \times l$ weighting matrix $\mathbf{Q}(j\omega)$. This study assumes that inaccessible states cannot be reconstructed via the use of Luenberger observers or other estimators due to design requirements. The desired $\mathbf{Q}(j\omega)$ is given as the "optimal" solution to

$$\mathbf{P_e}(j\omega) = \mathbf{P}(j\omega)\mathbf{Q}(j\omega) \tag{1.1}$$

Synthesis of a QFT design for a given nonsquare plant transfer matrix $\mathbf{P}(j\omega)$ is not begun until after the weighting matrix $\mathbf{Q}(j\omega)$ is determined. Since the selection process of $\mathbf{Q}(j\omega)$ is not an inherent part of performing a QFT design, the use of a $\mathbf{Q}(j\omega)$ weighting matrix should increase design freedom.

It is anticipated that properly selecting the $\mathbf{Q}(j\omega)$ matrix yields a product matrix $\mathbf{P}(j\omega)\mathbf{Q}(j\omega)$ whose determinant is MP over all plant parameter variations

and whose QFT-designed closed-loop performance is better than that achievable by squaring down $\mathbf{P}(j\omega)$ without the use of any optimization criteria. Improvements are expected because the $\mathbf{Q}(j\omega)$ weighting matrix acts as a control input mixer to coordinate efforts of different control inputs in order to increase the overall effectiveness of these inputs in achieving desirable plant responses.

Different optimization criteria for use in determining a $\mathbf{Q}(j\omega)$ for noninvertible $\mathbf{P}(j\omega)$ matrices are examined. A single QFT design problem is examined. While the completion of a QFT design was desired, the design is not completed because of problems encountered.

1.1 *Background*

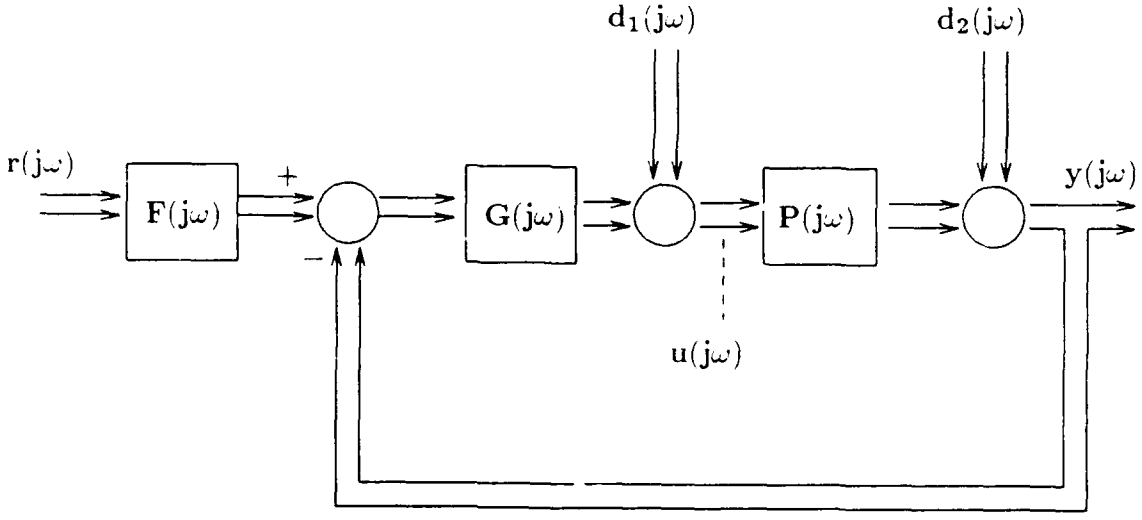

Figure 1.1. The QFT Compensated Plant

Figure 1.1 shows the QFT design matrices that are inserted as a result of synthesizing a QFT design on an $l \times l$ plant matrix. For purposes of this study, all system elements are assumed to be expressed in the frequency domain. The system elements are defined as follows:

$\mathbf{u}(j\omega)$ is the control surface command input as seen by the aircraft plant.

$\mathbf{r}(j\omega)$ is the aircraft command control input provided by an external source.

$\mathbf{y}(j\omega)$ is the aircraft plant output.

$\mathbf{d_1}(j\omega)$ and $\mathbf{d_2}(j\omega)$ are disturbance inputs.

$\mathbf{P}(j\omega)$ is the uncompensated plant matrix.

$\mathbf{F}(j\omega)$ is the QFT determined input filter or prefilter.

$\mathbf{G}(j\omega)$ is the QFT determined cascade compensator.

For the QFT design problem, the output $\mathbf{y}(j\omega)$ is required to track the command input $\mathbf{r}(j\omega)$ and to reject the disturbances $\mathbf{d_1}(j\omega)$ and $\mathbf{d_2}(j\omega)$. The $\mathbf{F}(j\omega)$ and $\mathbf{G}(j\omega)$ elements are designed to ensure that the sensitivity of the output to uncertainties in $\mathbf{P}(j\omega)$ is acceptable and to attentuate the effects of the two disturbance inputs. In addition, $\mathbf{F}(j\omega)$ is also designed to achieve an acceptable tracking response. The actual design and the cost of feedback are closely related to the extent of plant uncertainties and to the narrowness of the performance tolerances (7:1.2-1.3). If a QFT design is performed using $\mathbf{d_1}(j\omega) = 0$, then the design problem is referred to as a type 2 disturbance problem. Similarly if a QFT design is performed using $\mathbf{d_2}(j\omega) = 0$, then the design problem is referred to as a type 1 disturbance problem.

Figure 1.2 reflects the use of a $\mathbf{Q}(j\omega)$ weighting matrix with a nonsquare plant matrix $\mathbf{P}(j\omega)$. A QFT design for the MIMO system of Figure 1.2 is executed on the product $\mathbf{P}(j\omega)\mathbf{Q}(j\omega)$. As such, type 1 disturbance problems are defined with $\mathbf{d_1}(j\omega)$ situated between $\mathbf{Q}(j\omega)$ and the $\mathbf{G}(j\omega)$ compensator. Equation (1.1) is established on the basis of the open loop transfer function between $\mathbf{u}'(j\omega)$ and $\mathbf{y}(j\omega)$ which is given by

$$\mathbf{y}(j\omega) = \mathbf{P}(j\omega)\mathbf{Q}(j\omega)\mathbf{u}'(j\omega) = \mathbf{P_e}(j\omega)\mathbf{u}'(j\omega)$$

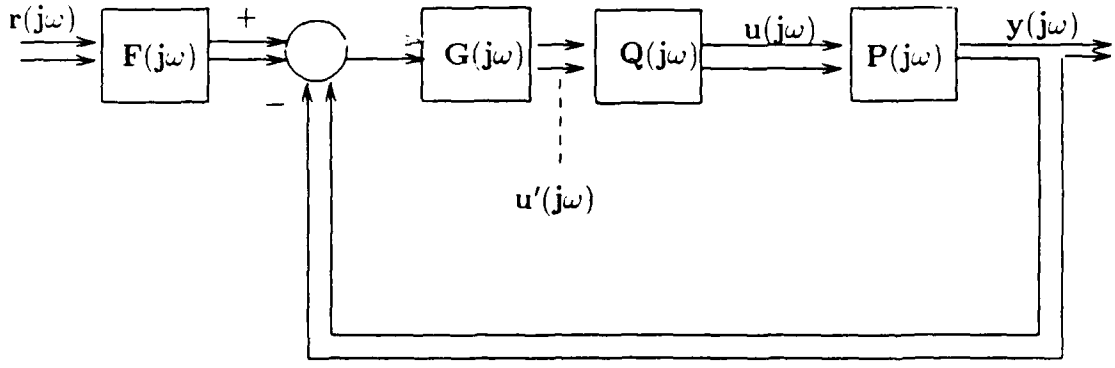

Figure 1.2. The QFT Compensated Plant with Added Weighting Matrix

A $\mathbf{Q}(j\omega)$ that minimizes the difference between the two sides of Equation (1.1) with respect to some criteria is desired.

The selection of elements for the $\mathbf{Q}(j\omega)$ matrix is not as straightforward as it may seem; the selection process is complicated by the existence of structured uncertainties in $\mathbf{P}(j\omega)$. By structured uncertainties, it is meant that transfer function elements of $\mathbf{P}(j\omega)$ vary so that the plant is actually described as a set of plants. Conversely, unstructured uncertainties are modeled by only specifying boundary conditions on the magnitude of plant deviations. The set of possible plants is denoted by $\mathcal{P}(j\omega)$. Each structured parameter variation in $\mathbf{P}(j\omega)$ potentially creates a new plant $\mathbf{P}(j\omega) \in \mathcal{P}(j\omega)$. If the structured plant variations occur over some continuous region, then the resultant set of plants is infinite. The objective of the QFT design process is then to satisfy design specifications for the set of all plants within the region defined by the structured uncertainties.

Past weighting matrix designs have generally sought to select elements of $\mathbf{Q}(j\omega)$ using engineering judgement and guesswork based on the physical characteristics of the plant and the importance of p_{ij} elements of $\mathbf{P}(j\omega)$ to the achievement of desirable outputs. Early attempts in determining $\mathbf{Q}(j\omega)$ concentrated on a $\mathbf{Q}(j\omega)$ of

constants only (1, 16). Later attempts by Hamilton and Phillips employed frequency dependent q_{ij} elements in their $\mathbf{Q}(j\omega)$ (12, 6). Selection methods for the transfer matrix elements of $\mathbf{Q}(j\omega)$, however, remained a matter of engineering judgement (i.e., trial and error). For the trial and error methods previously attempted, closed-loop performance results have generally served to differentiate between effective and ineffective choices for the matrix elements of $\mathbf{Q}(j\omega)$.

Additional work is needed to better define selection criteria for elements of the frequency sensitive weighting matrix $\mathbf{Q}(j\omega)$. Improvements in optimizing the selection of $\mathbf{Q}(j\omega)$ can also be applied to other MIMO design techniques that use weighting matrices. An example of such is Porter and Manganas' digital control design technique that first squares-down a non-square plant matrix into an equivalent square matrix (13). A squaring-down technique was used by Phillips in his study (12).

1.2 *Problem Statement*

This thesis examines the use of H_2 and H_∞-norm minimization as desirable criteria for defining an optimal $\mathbf{Q}(j\omega)$ compensator to Equation (1.1) for a plant matrix $\mathbf{P}(j\omega)$ with structured uncertainties subject to disturbances $\mathbf{d_1}(j\omega)$ and $\mathbf{d_2}(j\omega)$ under the assumptions that: 1) inaccessible states cannot be reconstructed, 2) $\mathbf{P}(j\omega)$ has more control inputs than outputs available for feedback, and 3) that the desirable plant matrix $\mathbf{P_e}(j\omega)$ is prespecified. This thesis then examines a design problem for roll rate and yaw rate tracking controllers for a linearized model of the AFTI/F16 aircraft.

1.3 *Review of Current Literature*

Quantitative feedback theory is essentially a frequency domain technique that emphasizes the use of feedback for achieving desired system performance levels despite plant disturbances and structured plant uncertainties. Specifics concerning the

theoretical basis of QFT and problem applications are available in (3, 7, 9, 22). The design technique is applicable to discrete and continuous systems for the following types of problems defined in (3:686-695):

1. Single-input, single-output (SISO) linear time-invariant (LTI) systems,
2. SISO nonlinear systems which are converted to equivalent SISO problems by first determining an LTI system that yields an equivalent set of permissible outputs over the set of all possible plants, disturbances, and inputs,
3. Multiple-input, multiple-output (MIMO) LTI systems which are solved as a set of equivalent multiple-input, single-output (MISO) systems,
4. MIMO nonlinear systems which are first converted to a MIMO LTI problem via the same methods used to convert SISO nonlinear problems to SISO LTI problems,
5. Distributed systems.

The use of QFT does not require approximations, linearizations via perturbation models, or the use of describing functions (9:86).

In each of the above five types of problems, solutions to satisfy design parameters are guaranteed to exist whenever appropriate QFT criteria are satisfied. One such condition is that the uncertainty in $\mathbf{P}(j\omega)$ be known or at least bounded (3:695). Additional conditions apply and are discussed in this study. It is noteworthy to indicate that QFT designs have been successfully applied to plants for which a subset of the set of all possible uncompensated plants were unstable or nonminimum-phase (NMP) (9, 7).

For nonsquare plants, the feedback control system of Figure 1.2 is the simplest of many possible schemes. Horowitz, et al, have suggested several multiple loop structures that further reduce disturbance impacts and system bandwidths in order to cope with large plant uncertainties. However, while such multiple loop structures

outperform single-loop feedback structures, the potential for introducing additional noise sources and for requiring plant modifications to implement the design are inherent drawbacks in the use of multiple-loop feedback structures (9:31-35).

Recently, Yaniv reexamined the MIMO design case (21). He suggested the following: "in each design step, say Step m, guarantee that $(1 + L_m(l))$ has no [right half plane] RHP zeros for all $l \in [1, ..., m]$; i.e., the same g_m designed in step m should also stabilize the systems $(1+L_m(1)), (1+L_m(2)), ..., (1+L_m(m))$. $G = diag(g_{ii})$ and $F = diag(f_{ii})$ will then be the solution to the problem stated ...." Implementing the change in the design procedure ensures that all resultant diagonal elements of the closed-loop transfer matrix have no RHP zeros, thus ensuring that the compensated system has minimum-phase properties. The L_i loop transmission functions are the $L_i = v_{ii}g_{ii}$ of Chapter II. If the loop transmission functions have no RHP zeroes, then the closed-loop functions of the compensated plant are minimum phase (MP). Yaniv's suggestion applies to plants that are basically non-interacting (BNIC). A plant is BNIC when it is highly diagonally dominant. In such cases, the use of a diagonal $\mathbf{F}(j\omega)$ matrix in the QFT design process is appropriate.

1.3.1 *Model Matching* In order to accomplish the stated objectives - to examine the use of H_2 and H_∞-norm minimization as desirable criteria for defining an optimal $\mathbf{Q}(j\omega)$ compensator to Equation (1.1) - it is necessary to examine a standard problem referred to as the model-matching problem. To this end, the bilateral model-matching problem is established and then related to Equation (1.1) by redefining elements of the model-matching problem.

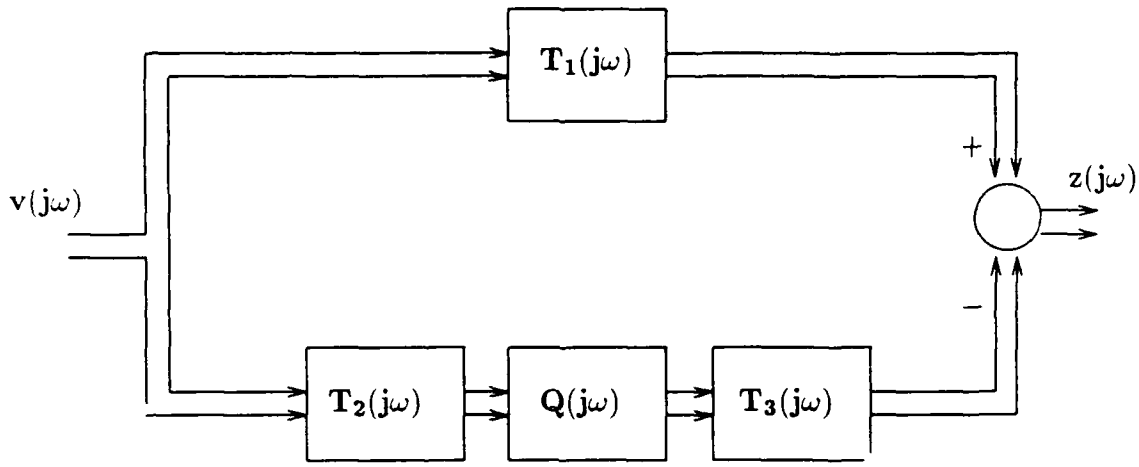

Figure 1.3. Model Matching Problem

Figure 1.3 is the model-matching problem set-up, where each of the $\mathbf{T}_i(j\omega)$, $i \in (1,2,3)$ are fixed and $\mathbf{Q}(j\omega)$ is an unknown compensator matrix.

The objective of model-matching is to design a stable controller $\mathbf{Q}(j\omega)$ that minimizes the difference between the input-output responses of $\mathbf{T_1}(j\omega)$ and the cascaded $\mathbf{T_2}(j\omega)$, $\mathbf{Q}(j\omega)$, and $\mathbf{T_3}(j\omega)$ transfer matrices. Depending on the model-matching criterion used, the problem is defined to either minimize the energy of the error $\mathbf{z}(j\omega)$ for the worst possible input $\mathbf{v}(j\omega)$ or to minimize the largest error in the magnitude of $\mathbf{z}(j\omega)$ for the worst possible input $\mathbf{v}(j\omega)$. In the first case, the problem is termed an H_2-norm minimization problem, while in the latter case it is termed an H_∞-norm minimization problem. The minimization requirement is given by the following equation.

$$\inf_{Q \in RH_\infty} \|\mathbf{\Phi}(j\omega)\|_{2,\infty} = \inf_{Q \in RH_\infty} \|\mathbf{T_1}(j\omega) - \mathbf{T_2}(j\omega)\mathbf{Q}(j\omega)\mathbf{T_3}(j\omega)\|_{2,\infty} \qquad (1.2)$$

where inf is the infimum for $\mathbf{Q}(j\omega)$ in the space of real rational, proper stable transfer functions. To be proper, the order of the numerator polynomial of $\mathbf{Q}(j\omega)$ is less than or equal to the order of the denominator polynomial. To be real rational, the transfer functions of $\mathbf{Q}(j\omega)$ must be expressible as a finite ratio of polynomials in $j\omega$ with real constants.

Solutions to the model-matching problem play an important role in H_2 and H_∞-norm optimization (see, for example (5)). However, because this study is directly interested with the model-matching problem, no effort is made to go into H_2 and H_∞-norm optimization theory.

For this study the model-matching problem is applied to the QFT problem of determining an optimal $\mathbf{Q}(j\omega)$ with respect to Equation (1.1) by redefining $\mathbf{T_1}(j\omega) = \mathbf{P_e}(j\omega)$, $\mathbf{T_2}(j\omega) = \mathbf{P}(j\omega)$, and $\mathbf{T_3}(j\omega) = I$. To do so however, requires that transfer function elements of $\mathbf{P_e}(j\omega)$ be stable (else, $\mathbf{P_e}(j\omega)$ is in neither of the two Hardy spaces of interest and norm-minimization is not applicable). Also note that for structured uncertainty problems, H_2-norm minimization is generally considered more appropriate than the use of H_∞-norm minimization.

1.4 Assumptions

The following assumptions are made.

It is assumed that the designer has either a linear state space model of the system or can establish an LTI equivalent. A linear state space model is of the form

$$\dot{x} = Ax + Bu \tag{1.3}$$

$$y = Cx + Du \tag{1.4}$$

where the A, B, C, and D elements of the equation are real matrices, and x, y, and u are vectors.

An LTI equivalent for most nonlinear plants can be determined for the purposes of QFT designs. The LTI equivalent plant is basically established by determining nonlinear system outputs as a function of system inputs at particular frequencies and then calculating that equivalent set of linear plants that produce comparable outputs under similar input conditions and for the given particular frequencies. An outline for determining LTI equivalent plants, and conditions for their solvability is given by Horowitz, et al, in (9:36–44).

The AFTI/F16 aircraft control example used in this study is developed under the following assumptions:

1. Aircraft equations of motions are linearized about the nominal equilibrium (trim) condition of Mach 0.9 at 20,000 feet. The model is assumed valid for *small perturbations about the nominal conditions.* **No effort is made to determine aircraft performance in regions outside the restrictions imposed by the model.**
2. Mass of aircraft remains constant.
3. Aircraft is symmetrical with reference to a vertical plane aligned with the longtitudinal axis of the aircraft.
4. Aircraft thrust remains constant.
5. Earth origin is taken as an acceptable inertial reference.
6. Atmosphere is a homogeneous mixture at rest with respect to the earth.
7. Dimensional stability derivatives are constant for the given flight and surface failure conditions modeled.

8. Control system failures can be described by scaling the elements of the B matrix. A reduction in the magnitude of elements of the B matrix is used to represent gradual loss of control surface effectiveness.

   (a) The portion of the control surface that has failed is assumed locked in the position associated with a trim flight condition.

   (b) Surface failures are assumed to provide no other impact on flight dynamics other than a reduction in the effectiveness of the control surface.

   (c) Control surface failures are assummed to not impact aircraft stability; that is, with control surface failures modeled by scaling columns of the B matrix, the plant's characteristic equation does not change.

9. The dynamic behavior of the plant's components in response to inputs is assumed describable by finite-dimensional Laplace transfer functions. See (12, 10).

10. Sensor characteristics are such that, for QFT design purposes, the problem can be modeled as a type 2 disturbance problem.

1.5 *Plan of Approach*

The following is the plan of approach for this study:

1. A linearized plant model is selected for problem study. The plant model has three inputs (aileron, rudder, and horizontal tail deflections) and three outputs of interest (sideslip angle β, roll rate p, and yaw rate r). The objective of the design is to provide roll and yaw rate responses that satisfy class IV aircraft level 1 flying qualities (4:412). For purposes of this study, sideslip is not available for feedback.

2. Using the performance objectives specified in Chapter III, a desirable plant $\mathbf{P}_e(j\omega)$ is selected to satisfy desirable plant characteristics described in (3) and

(7) and design criteria in (4:412). The objective is to determine a $\mathbf{Q}(j\omega)$, such that

(a) The product of $\mathbf{P}(j\omega)$ and $\mathbf{Q}(j\omega)$ is a square matrix.

(b) The product $\mathbf{P}(j\omega)\mathbf{Q}(j\omega)$ is non-singular over the entire range of plant uncertainties. Letting $\mathcal{P}_e(j\omega)$ be the set of all equivalent plants formed by the product $\mathbf{P}(j\omega)\mathbf{Q}(j\omega)$ for any $\mathbf{P}(j\omega) \in \mathcal{P}(j\omega)$, this condition is equivalently stated by requiring that $\mathcal{P}_e(j\omega)$ be nonsingular over the set of possible equivalent plants. Note that this condition is applied to the functions in $\mathbf{P}_e(j\omega) \in \mathcal{P}_e(j\omega)$ and not to evaluations of the functions at particular frequencies.

(c) The product $\mathbf{P}(j\omega)\mathbf{Q}(j\omega)$ satisfies a diagonal dominance condition over the range of plant uncertainties. This condition ensures that the diagonal transfer functions dominate the system's response to control inputs over the entire range of plant parameter variations in the high frequency range (i.e, above some cut-off frequency). As such the evaluation is conducted as $\omega \rightarrow \infty$. A more severe version of the diagonal dominance condition is Rosenbrock's diagonal dominance requirement. Rosenbrock's diagonal dominance requirement is, however, not a constraint that must be satisfied prior to seeking a QFT design.

(d) The poles of $\mathbf{P}_e^{-1}(j\omega)$ lie in the LHP over the range of plant uncertainties. In performing a QFT design, the m_{ij} elements of $\mathbf{P}_e^{-1}(j\omega)$ are individually inverted. As such, all poles of the m_{ij} must be in the LHP to guarantee that the m_{ij}^{-1} are MP. To satisfy this criteria requires that factors of the determinant $det(\mathbf{P}_e(j\omega))$ all lie in the LHP over the set of all possible plants.

3. The $\mathbf{P}_e(j\omega)$ chosen for use in the optimization part of this study is

$$\mathbf{P_e}(\mathbf{j}\omega) = \begin{pmatrix} p_{e_{11}} & p_{e_{12}} \\ p_{e_{21}} & p_{e_{22}} \end{pmatrix} \tag{1.5}$$

with

$$\begin{aligned} p_{e_{11}} &= 562.5/[(j\omega + 10)(-\omega^2 + 9j\omega + 56.25)] \\ p_{e_{12}} &= (j\omega + .001)/[(j\omega + 10)^2(-\omega^2 + 9j\omega + 56.25)] \\ p_{e_{21}} &= p_{e_{12}} \\ p_{e_{22}} &= p_{e_{11}} \end{aligned} \tag{1.6}$$

4. With $\mathbf{P_e}(\mathbf{j}\omega)$ specified, the $\mathbf{Q}(\mathbf{j}\omega)$ weighting matrix is determined in accordance with optimization selection criteria developed in Chapter II. The $\mathbf{Q}(\mathbf{j}\omega)$ matrix is of the format shown in the following equation with the q_{ij} being the transfer function elements of $\mathbf{Q}(\mathbf{j}\omega)$.

$$\mathbf{Q}(\mathbf{j}\omega) = \begin{pmatrix} q_{11} & q_{12} \\ q_{21} & q_{22} \\ q_{31} & q_{32} \end{pmatrix} \tag{1.7}$$

A QFT design is then performed using the product $\mathbf{P}(\mathbf{j}\omega)\mathbf{Q}(\mathbf{j}\omega)$. Design objective is to maintain class I roll and yaw performance handling qualities for the set of healthy and degraded plants. However, due to problems encountered,

this study was not able to obtain an acceptable $\mathbf{Q}(j\omega)$. As such a QFT design for the plant described and an evaluation of the design is not accomplished.

1.6 Scope

The method of specified outputs applies. The objective of the $\mathbf{Q}(j\omega)$ matrix is to minimize the difference between the original plant transfer matrix and a prespecified, more desirable equivalent plant matrix $\mathbf{P_e}(j\omega)$.

All analyses are performed in the frequency domain; digital considerations are not addressed. It is noted; however, that both quantitative feedback theory and H_2 and H_∞-norm minimization are applicable to both discrete and continuous functions. As such, criteria and methodologies examined in this study are applicable to discrete systems.

1.7 Presentation

Chapter II provides an overview of pertinent theoretical information. Sections of Chapter II address QFT theory while focusing on those plant properties that must be satisfied if a QFT design is to be attempted. Optimal means for determining $\mathbf{Q}(j\omega)$ are also examined.

Chapter III explores applications of QFT and weighting matrix selection criteria to a tracking problem using the lateral-directional model of the AFTI/F16. The selection of $\mathbf{P_e}(j\omega)$ and results concerning efforts to obtain $\mathbf{Q}(j\omega)$ are presented.

Chapter IV summarizes conclusions of this study and provides pertinent recommendations.

II. Theoretical Background

2.1 Introduction

The theoretical background for this study is presented as follows. First energy and power spectral density relationships both in the time and frequency domains are stated. Then, in order to provide a basis for subsequent discussions concerning singular values, the singular value decomposition of matrices of constants and matrices of functions in $j\omega$ are examined. An effort is made to determine the availability of transfer function descriptions for defining elements of the singular value decomposition of matrices of functions as a means of determining optimal solutions to the model-matching problem.

With the basics thus established, H_2 and H_∞-norm minimization definitions are made and relationships defined between the norm minimization criteria and the energy and power spectral densities. The Quantitative Feedback Technique is next examined; both the basis of the MISO equivalent QFT design method and the source of the QFT design criteria are established. Because of the importance of the minimum-phase property to QFT, the impact of nonminimum-phase plants and methods available for determining when a plant is NMP are next examined. In addition, each of these methods is examined in the context of its usefulness for establishing criteria in selecting $\mathbf{Q}(j\omega)$ weighting matrices that guarantee that the product $\mathbf{P}(j\omega)\mathbf{Q}(j\omega)$ is MP for all plant parameter variations.

Finally, each of the QFT design criteria is reexamined with the goal of determining how the criteria impact the selection of the frequency sensitive weighting matrix $\mathbf{Q}(j\omega)$ and how H_2 and H_∞-norms can be used to define a $\mathbf{Q}(j\omega)$ that is optimal with respect to Equation (1.1) whenever transfer function elements of $\mathbf{P}(j\omega)$ are known stable for all plant parameter variations.

2.2 *Spectral Functions*

Equation 2.1 represents the function of time $p(t)$ as a continuous sum of scalar exponential functions of frequency $\mathbf{p}(\mathbf{j}\omega)$; $\mathbf{p}(\mathbf{j}\omega)$ is the Fourier transform or *Fourier spectrum* of $p(t)$. The relationship between $p(t)$ and $\mathbf{p}(\mathbf{j}\omega)$ is [1]

$$p(t) = \frac{1}{2\pi}\int_{-\infty}^{\infty} \mathbf{p}(\mathbf{j}\omega)e^{j\omega t}d\omega \tag{2.1}$$

$$\mathbf{p}(\mathbf{j}\omega) = \int_{-\infty}^{\infty} p(t)e^{-j\omega t}dt \tag{2.2}$$

A signal of finite energy can be described by a continuous spectral-density function by obtaining the Fourier transform of the signal (Equation (2.2)). The Fourier transform of the signal, in turn, can be found by setting $s = j\omega$ in the Laplace transform of $p(t)$, whenever both of the following conditions are true.

1. $p(t) = 0$ for $t < 0$, and
2. $p(t)$ has finite energy, that is, $\int_{-\infty}^{\infty} |p(t)|^2 dt < \infty$.

Since it is assumed that all functions of time used in this study satisfy the above conditions , the function $\mathbf{p}(\mathbf{j}\omega)$ is obtainable by substituting $j\omega$ for s in the Laplace transform of $p(t)$. As a result, while all functions in the remainder of this chapter are functions either of time t or frequency ω, the existence of the Laplace transforms of $p(t)$ is assumed in order to obtain $\mathbf{p}(\mathbf{j}\omega)$.

In contrast to continuous functions, periodic waveforms and the dc components of a signal have all of their amplitude components at discrete frequencies. To portray the amplitude components of a periodic waveform on a spectral density graph

[1] The most common convention in defining the transform coefficients is in use here. See (11:110-112).

requires the use of impulse functions. The area (weight) of an impulse is the magnitude of the time function's amplitude and the spectral position of that component is the frequency at which the impulse occurs. (18:83-84).

If a signal $p(t)$ represents a voltage, then $\mathbf{p}(\mathbf{j}\omega)$ has dimensions of voltage multiplied by time. The area under the spectral density function $\mathbf{p}(\mathbf{j}\omega)$, therefore, has dimensions of voltage because frequency has dimensions of inverse time. Each point on a plot of $\mathbf{p}(\mathbf{j}\omega)$ versus ω indicates the relative weighting of each frequency component. As such, plots of $\mathbf{p}(\mathbf{j}\omega)$ versus ω can be considered as density functions. The contribution of a given frequency band to the representation of $p(t)$ is found by integrating $\mathbf{p}(\mathbf{j}\omega)$ over the bandwidth area.

The square of the absolute value of $p(t)$ is called the *energy spectral density* or energy spectrum of $p(t)$. From the mathematics of the Fourier integral, and both Rayleigh's and Parseval's theorems (18:85), the energy of a signal E is given by

$$\begin{aligned} E &= \int_{-\infty}^{\infty} |p(t)|^2 dt \\ &= \frac{1}{2\pi} \int_{-\infty}^{\infty} \overline{\mathbf{p}}(\mathbf{j}\omega)\mathbf{p}(\mathbf{j}\omega)\mathbf{d}\omega \\ &= \frac{1}{2\pi} \int_{-\infty}^{\infty} |\mathbf{p}(\mathbf{j}\omega)|^2 \mathbf{d}\omega \end{aligned} \tag{2.3}$$

In this thesis, only real valued functions of time are considered. Thus, $|p(t)|^2 = p^2(t)$. By examining Equation (2.3), it is seen that the energy spectral density is expressible in either the time or frequency domain. Energy contributions of a given frequency band are found by integrating over the desired bandwidth. The total system energy E is found by integrating over $(-\infty, \infty)$. Since the energy spectral densities of real valued signals are even, E is also twice the value found by integrating $\mathbf{p}(\mathbf{j}\omega)$ over the interval $[0, \infty)$.

In the metric system of units, energy E is measured in joules. Hence, the units of the energy density in the time domain must be (joules)^2/ second and in the frequency domain (joules)^2/ Hertz.

Table 2.1 lists common energy-storage elements that exist in physical systems, and the corresponding energy equations for E. The table provides insight into the use of spectral energy density functions in units other than voltage. Table data is extracted from (3). In the generalized sense, energy density expressions are given as (quantity)^2/ Hertz.

Table 2.1. Energy-storage Elements

Element	Energy	Variable
Capacitor C	$\frac{Cv^2}{2}$	Voltage v
Inductor L	$\frac{Li^2}{2}$	Current i
Mass M	$\frac{Mv^2}{2}$	Translational Velocity v
Moment of Inertia J	$\frac{J\omega^2}{2}$	Rotational Velocity ω
Spring K	$\frac{Kx^2}{2}$	Displacement x

For many applications, the *power spectral density* or power spectrum is of more interest than the energy spectrum. To describe differences between the energy and power spectral densities first requires an explanation of the characterictics of energy and power signals.

An energy signal is one that: (1) has finite energy content, (2) zero average power (since the finite energy content over infinite time yields zero), and whose form is non-periodic and deterministic. A power signal, on the other hand, is one that: (1) has finite average power, (2) infinite energy, and (3) whose form is that of either a periodic or random signal extending infinitely over time.

Since energy and power signals are inherently different, it follows that the functions describing energy and power versus time or frequency are different for the

two types of signals.

The time-averaged power of a signal is given by (18:156)

$$P_f = \lim_{T \to \infty} \frac{1}{T} \int_{\frac{-T}{2}}^{\frac{T}{2}} p^2(t) dt \tag{2.4}$$

In a manner analagous with the definition of the energy E through the use of the energy spectral density, the time-averaged power is defined in terms of a power spectral density $\mathbf{S_f}(\mathbf{j}\omega)$ by

$$P_f = \frac{1}{2\pi} \int_{-\infty}^{\infty} \mathbf{S_f}(\mathbf{j}\omega) \mathbf{d}\omega \tag{2.5}$$

For both random and deterministic signals whose power spectral densities do not vary with time, the power spectral density function is obtained by taking the Fourier transform of the autocorrelation function. The autocorrelation function $R_f(\tau)$ (18:168–169) is given as

$$R_f(\tau) = \lim_{T \to \infty} \frac{1}{T} \int_{\frac{-T}{2}}^{\frac{T}{2}} p(t+\tau) p(t)\, dt \tag{2.6}$$

with $\mathbf{S_f}(\mathbf{j}\omega)$ in Equation (2.5) given as $\mathbf{S_f}(\mathbf{j}\omega) = \int_{-\infty}^{\infty} \mathbf{R_f}(\tau) \mathbf{e}^{-\mathbf{j}\omega\tau} \mathbf{d}\tau$. For random, stationary signals (i.e., random signals whose statistics do not change as a function of time), the autocorrelation function is given by

$$R_f(\tau) = E\{p(t)p(t+\tau)\} \tag{2.7}$$

where $R_f(\tau)$ is found by time averaging (taking the expectation of) a statistical function assumed to be ergodic (functions whose characteristics are such that time averaging a single signal yields the same statistics as obtaining the ensemble average; note that ergodicity, in turn, implies stationarity (but not vice versa)) (18:471-480). Certain nonperiodic power signals are not Fourier transformable; in such cases the power spectral density of the signal is expressed in a "limiting" sense (18:488-490).

Power spectral densities of periodic and random signals are real, even, and nonnegative functions of frequency. In the metric system of units, the power P_f is measured in watts. Hence, the units of the power density are watts/Hertz for $\mathbf{S_f}(j\omega)$.

2.3 *Singular Value Decompositions of Matrices of Constants*

The factorization of a real symmetric matrix P into $P = U\Sigma U^T$, $UU^T = I$, and with the eigenvalues of P in the diagonal matrix Σ, is known as the spectral theorem. The matrix U is termed unitary, eigenvectors of U are orthonormal. The key to understanding the relationship between singular value decomposition (which applies to real symmetric matrices) and the spectral theorem (which applies to any matrix P) is to recognize that the matrix products PP^T and P^TP are always symmetric.

The singular value decomposition theorem provides that any real $l \times m$ matrix P can be factored into $P = U\Sigma V^T$ = (unitary)(diagonal)(unitary), where columns of U ($l \times l$) are eigenvectors of PP^T, columns of V ($m \times m$) are eigenvectors of P^TP, and where the diagonal entries of Σ ($l \times m$) are the real, non-negative values that are termed the singular values of P. For complex matrices, Σ is real and both U and V are unitary (i.e., $U^*U = I$ and $V^*V = I$ where $(.)^*$ is the conjugate transpose operation) (17:298,442–443). Note that for nonsquare P, Σ is nonsquare.

For example, consider

$$P = \begin{pmatrix} 1+2j & 2+3j & 3+4j \\ 4-j & 5-j & 6-j \end{pmatrix}$$

The singular value decomposition for $P = U\Sigma V^*$ is given by

$$U = \begin{pmatrix} 0.3331 + 0.4864j & 0.7322 + 0.3411j \\ 0.7931 - 0.1533j & -0.4411 + 0.3911j \end{pmatrix}$$

$$\Sigma = \begin{pmatrix} 11.0528 & 0 & 0 \\ 0 & 0.9137 & 0 \end{pmatrix}$$

$$V^* = \begin{pmatrix} 0.4190 & 0.5649 & 0.7108 \\ -0.8110 & -0.1191 & 0.5728 \\ 0.4082 & -0.8165 & 0.4082 \end{pmatrix}$$

A connection between PP^* and P^*P is evident. The eigenvalues of PP^* and P^*P are the same. This is readily seen by observing that substitution of the singular value decomposition of P into PP^* and P^*P results in eigenvalue-preserving similarity transformations.

$$\begin{aligned} PP^* &= U\Sigma V^* (U\Sigma V^*)^* \\ &= U\Sigma\Sigma^* U^* \end{aligned} \tag{2.8}$$

and similarly,

$$\begin{aligned} P^*P &= (U\Sigma V^*)^* U\Sigma V^* \\ &= V\Sigma^*\Sigma V^* \end{aligned} \tag{2.9}$$

so that in each case, similarity transformations on either $\Sigma\Sigma^*$ or $\Sigma^*\Sigma$ are obtained.

Most applications involving singular value decompositions take advantage of the numerical stability inherent in performing calculations using the decomposed form of the P matrix. Computational stability is provided by the orthogonality of the U and V matrices since $x^*U^*Ux = x^*x$. However, such a statement cannot be made about Σ. Nevertheless, Σ is as accurate as possible, and it reveals the kind of numerical stability problems which can be encountered (17:444).

Another use of the singular value decomposition of a matrix P is in finding the pseudoinverse of P. The pseudoinverse of a matrix provides the minimum length projection solution to an inconsistent set of equations.

If the singular value decomposition of P is given as $P = U\Sigma V^*$, then the pseudoinverse of P, denoted as P^+, is (17:449)

$$P^+ = V\Sigma^+U^* \tag{2.10}$$

where the singular values of P are on the diagonal of Σ, and the reciprocals, in the same order, are on the diagonal of Σ^+.

Using the previous example in this section, the pseudoinverse of P is given as $P^+ = V\Sigma^+U^*$, where

$$V = \begin{pmatrix} 0.4190 & -0.8110 & 0.4082 \\ 0.5649 & -0.1191 & -0.8165 \\ 0.7108 & 0.5728 & 0.4082 \end{pmatrix}$$

$$\Sigma^{+} = \begin{pmatrix} \frac{1}{11.0528} & 0 \\ 0 & \frac{1}{.9137} \\ 0 & 0 \end{pmatrix}$$

$$U^{*} = \begin{pmatrix} 0.3331 - .4864j & 0.7931 + .1533j \\ 0.7322 - .3411j & -0.4411 - .3911j \end{pmatrix}$$

With these results established, the following claim is made. If B is any matrix whose nonzero singular values are the same as those of P, then there exists a transformation matrix T that satisfies $T^{*}B^{*}BT = P^{*}P$. This claim parallels the invariance of the characteristic equation of a square plant transfer matrix presented in (3:170).

Let $P = U_P \Sigma_P V_P^{*}$, and $B = U_B \Sigma_B V_B^{*}$ such that the nonzero singular values of $P^{*}P$ and $B^{*}B$ are equal. By assumption, one of the following cases applies:

case a: $\Sigma_P^{*}\Sigma_P = \Sigma_B^{*}\Sigma_B$

case b: $\Sigma_P^{*}\Sigma_P = \begin{pmatrix} \Sigma_B^{*}\Sigma_B & 0 \\ 0 & 0 \end{pmatrix}$

case c: $\Sigma_B^{*}\Sigma_B = \begin{pmatrix} \Sigma_P^{*}\Sigma_P & 0 \\ 0 & 0 \end{pmatrix}$

where the 0 submatrices are chosen to provide conformability between $\Sigma_P^{*}\Sigma_P$ and $\Sigma_B^{*}\Sigma_B$. If case a, then

$$
\begin{aligned}
\Sigma_B^* \Sigma_B &= \Sigma_P^* \Sigma_P \\
V_P \Sigma_B^* \Sigma_B V_P^* &= V_P \Sigma_P^* U_P^* U_P \Sigma_P V_P^* \\
V_P \Sigma_B^* \Sigma_B V_P^* &= P^* P \\
V_P V_B^* V_B \Sigma_B^* \Sigma_B V_B^* V_B V_P^* &= P^* P \\
V_P V_B^* B^* B V_B V_P^* &= P^* P
\end{aligned}
$$

Hence, select

$$T = V_B V_P^* \tag{2.11}$$

The desired transformations for cases b and c are similarly obtained.

2.4 *Singular Value Decompositions of* $\mathbf{P}(\mathbf{j}\omega)$ *Matrices*

Both MATRIX$_x$ and MACSYMA can be used to obtain singular value decompositions of matrices whose entries are constants. For example, the MATRIX$_x$ "SVD" command is used to obtain the singular value decomposition of any matrix of constants (8:4-27).

MACSYMA, however, is capable of performing numeric and symbolic manipulations. While MACSYMA has no command for directly obtaining the singular value decomposition of a matrix of transfer functions; the "unit eigenvectors" command is available for obtaining eigenvectors and eigenvalues of PP^* and P^*P needed to construct the U, Σ , and V^* matrices (19:12-14). In using MACSYMA, the Σ matrix is obtained as the matrix formed by placing the square root of eigenvalues of PP^*

along the diagonal. While MACSYMA appears to have the desired capability, it must be noted that for even a simple 2×3 test case using a matrix whose elements were of the form $a/(j\omega + b)$, with a and b constant, MACSYMA requires several processing hours and returns a solution that is extremely difficult to interpret. For more complex matrices, MACSYMA is unable to return the desired information because of the size of the polynomials involved in performing necessary calculations.

As such, if the singular value decomposition of a matrix of transfer functions $\mathbf{P}(\mathrm{j}\omega)$ is desired, it is necessary to use numerical means to estimate elements of the decomposition.

The method followed is to repeatedly obtain the singular value decomposition of a matrix $\mathbf{P}(\mathrm{j}\omega)$ evaluated at frequencies in an interval of interest. Points obtained using the pointwise decomposition of $\mathbf{P}(\mathrm{j}\omega)$ are then plotted to yield magnitude and phase plots of each element in $\mathbf{U}(\mathrm{j}\omega)$, $\mathbf{V}(\mathrm{j}\omega)$, and $\mathbf{\Sigma}(\omega)$. The objective is to then estimate the transfer function elements of each matrix element by using curve fitting approximations.

The following $\mathbf{P}(\mathrm{j}\omega)$ is used as a test case.

$$\mathbf{P}(\mathrm{j}\omega) = \begin{pmatrix} \frac{(j\omega-1)(j\omega+1)}{(j\omega+1)(j\omega+2)(j\omega+4)} & \frac{(j\omega+2)}{(j\omega+1)(j\omega+2)(j\omega+4)} & \frac{3}{(j\omega+1)(j\omega+2)(j\omega+4)} \\ 0 & \frac{(j\omega+2)(j\omega+3)}{(j\omega+1)(j\omega+2)(j\omega+4)} & \frac{(j\omega+4)}{(j\omega+1)(j\omega+2)(j\omega+4)} \end{pmatrix}$$

The matrix $\mathbf{P}(\mathrm{j}\omega)$ is evaluated at ω over the interval [.001, 1000] and results obtained (see Figures 2.1 through 2.5).

The continuous lines of Figure 2.1 are plots of the $\sigma_1(\omega)$ and $\sigma_2(\omega)$ transfer function elements of $\mathbf{\Sigma}(\omega)$ as a function of frequency ω (the dotted lines are approximations to the functions). The plot of $\sigma_1(\omega)$ is the upper plot of Figure 2.1 while that of $\sigma_2(\omega)$ is the lower plot. Each of the $\sigma_i(\omega)$ plots is a nonnegative function with zero phase for all ω. Note that a real-rational function in ω cannot be used

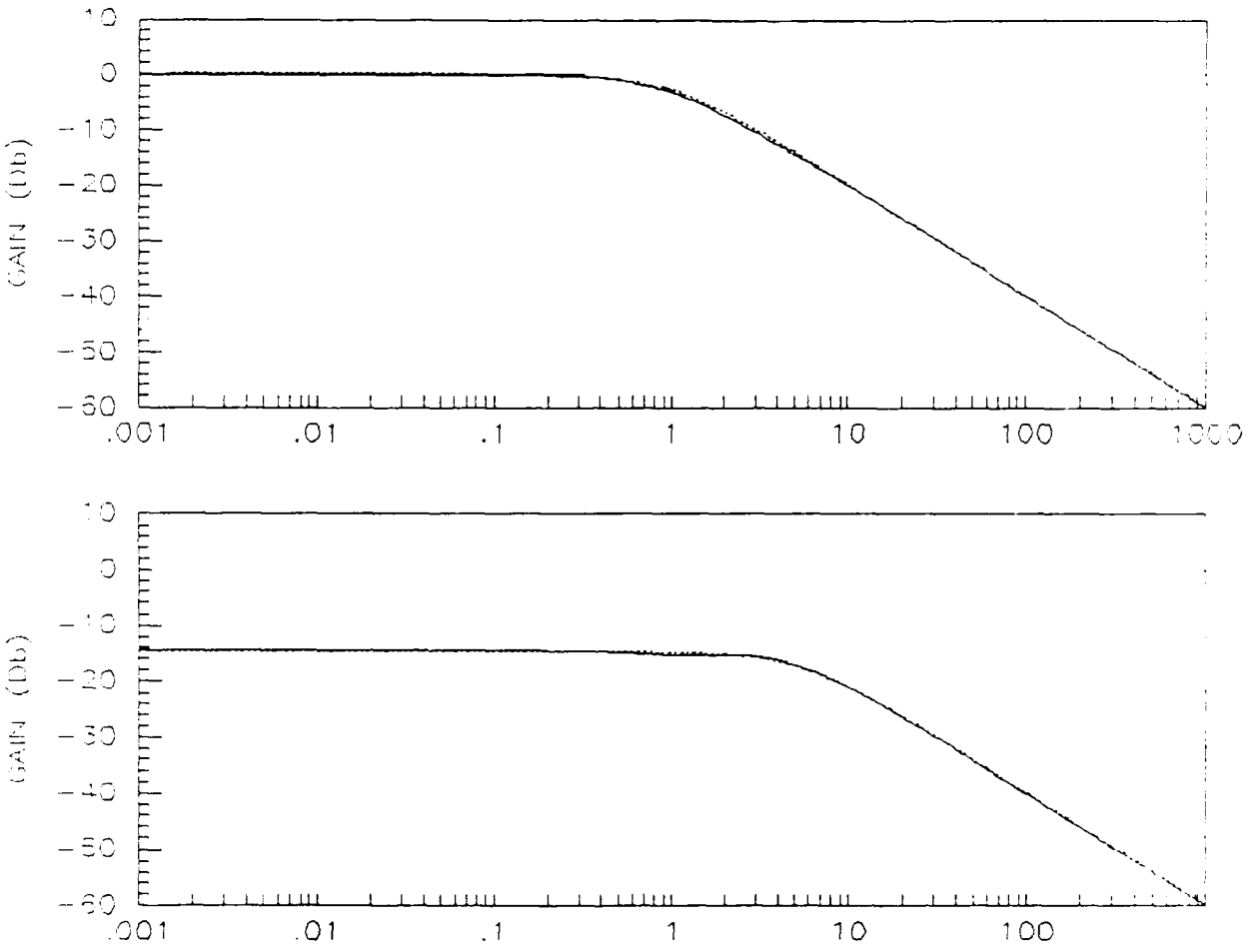

Figure 2.1. Plots of $\sigma_1(\omega)$ and $\sigma_2(\omega)$

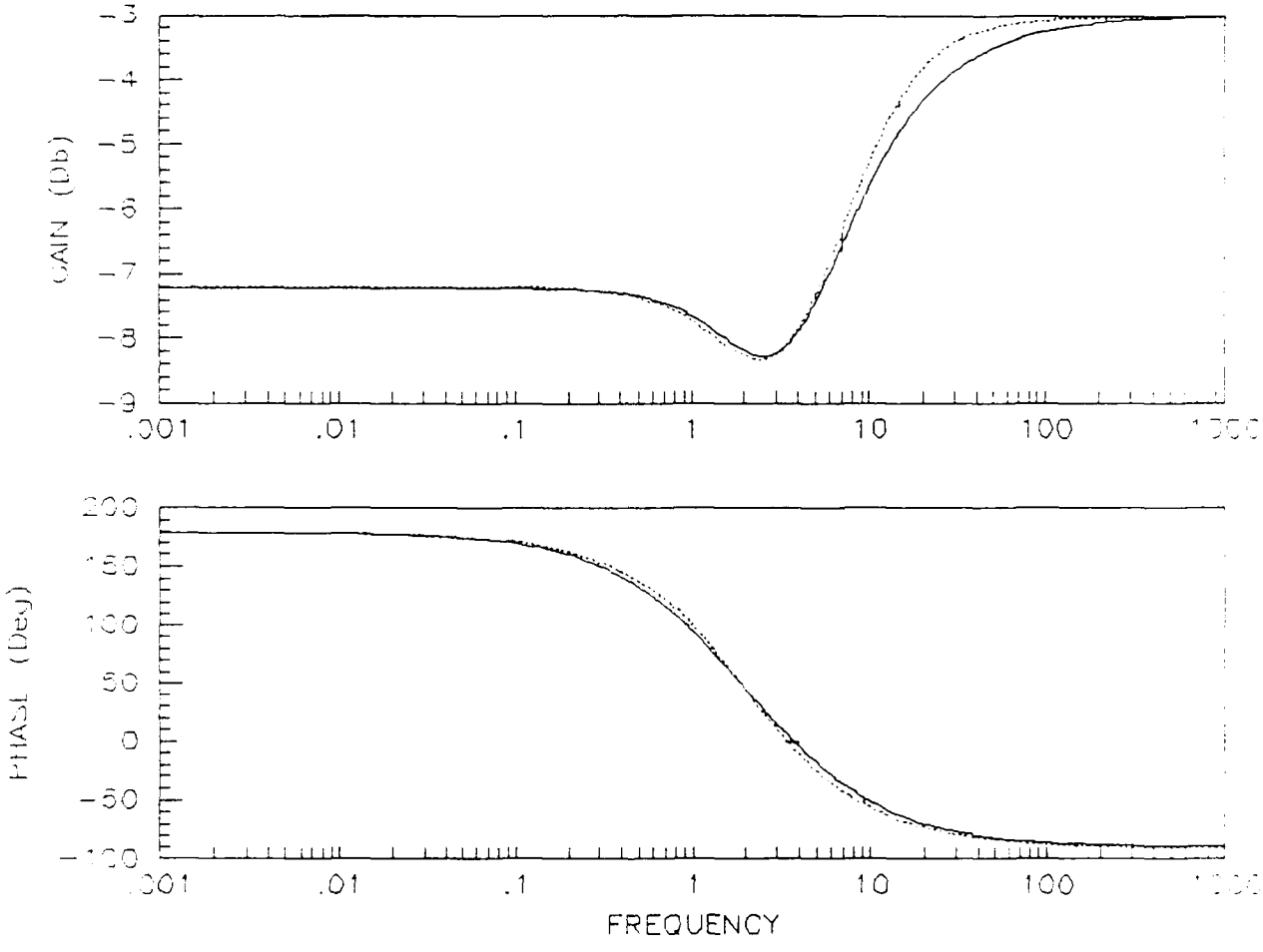

Figure 2.2. Plot of $\mathbf{u_{11}}(j\omega)$

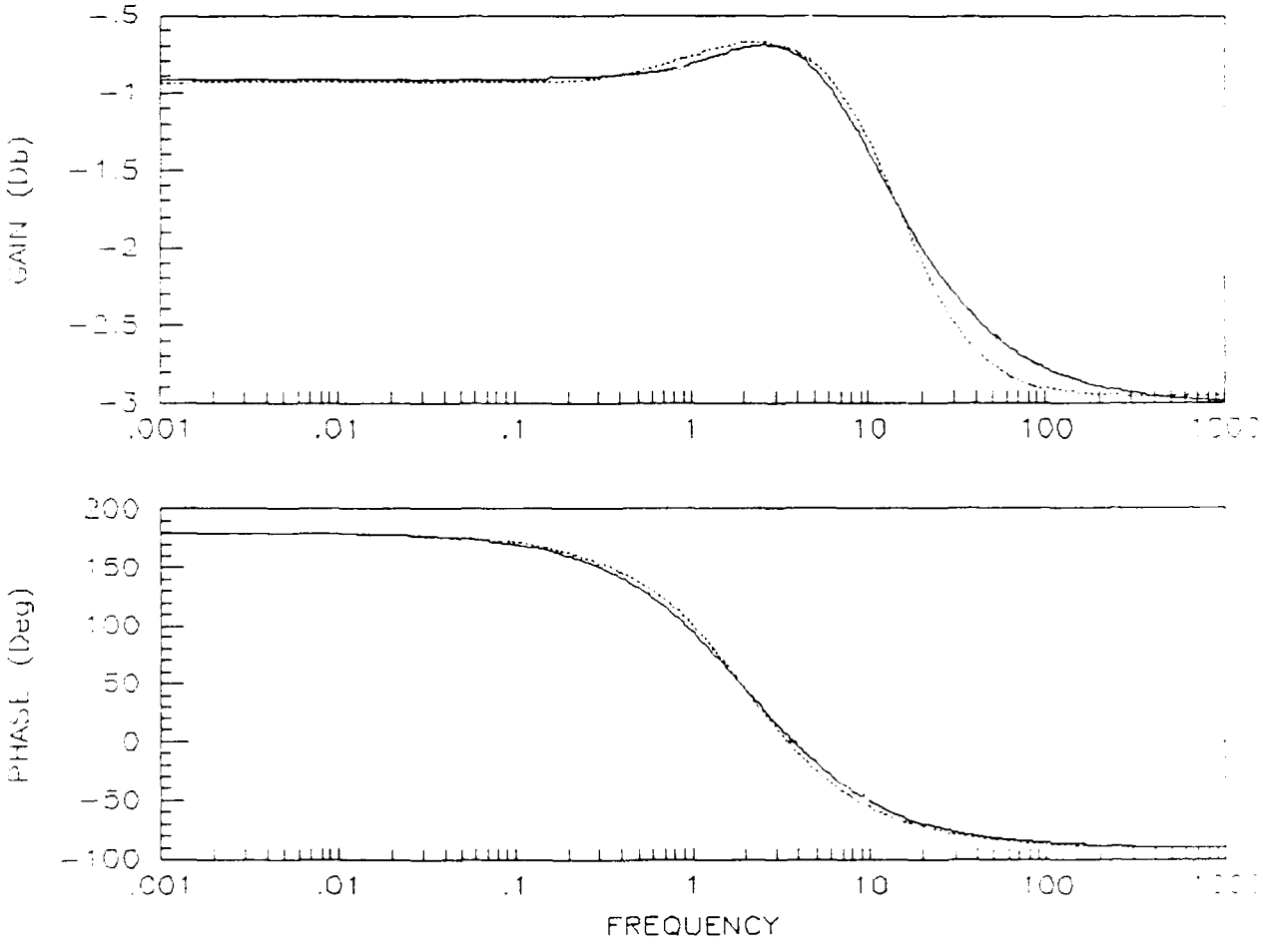

Figure 2.3. Plot of $\mathbf{u_{12}}(j\omega)$

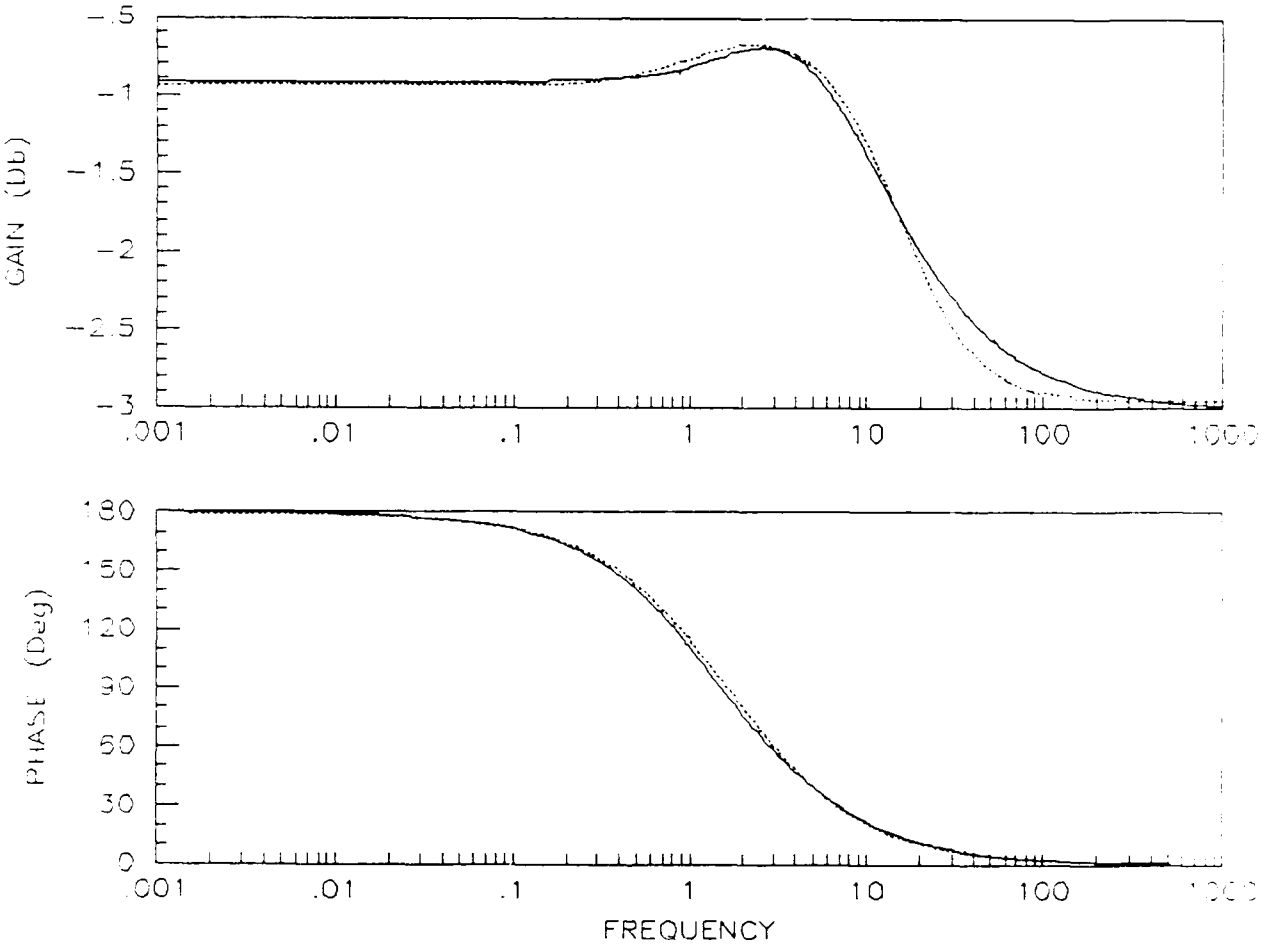

Figure 2.4. Plot of $\mathbf{u_{21}}(j\omega)$

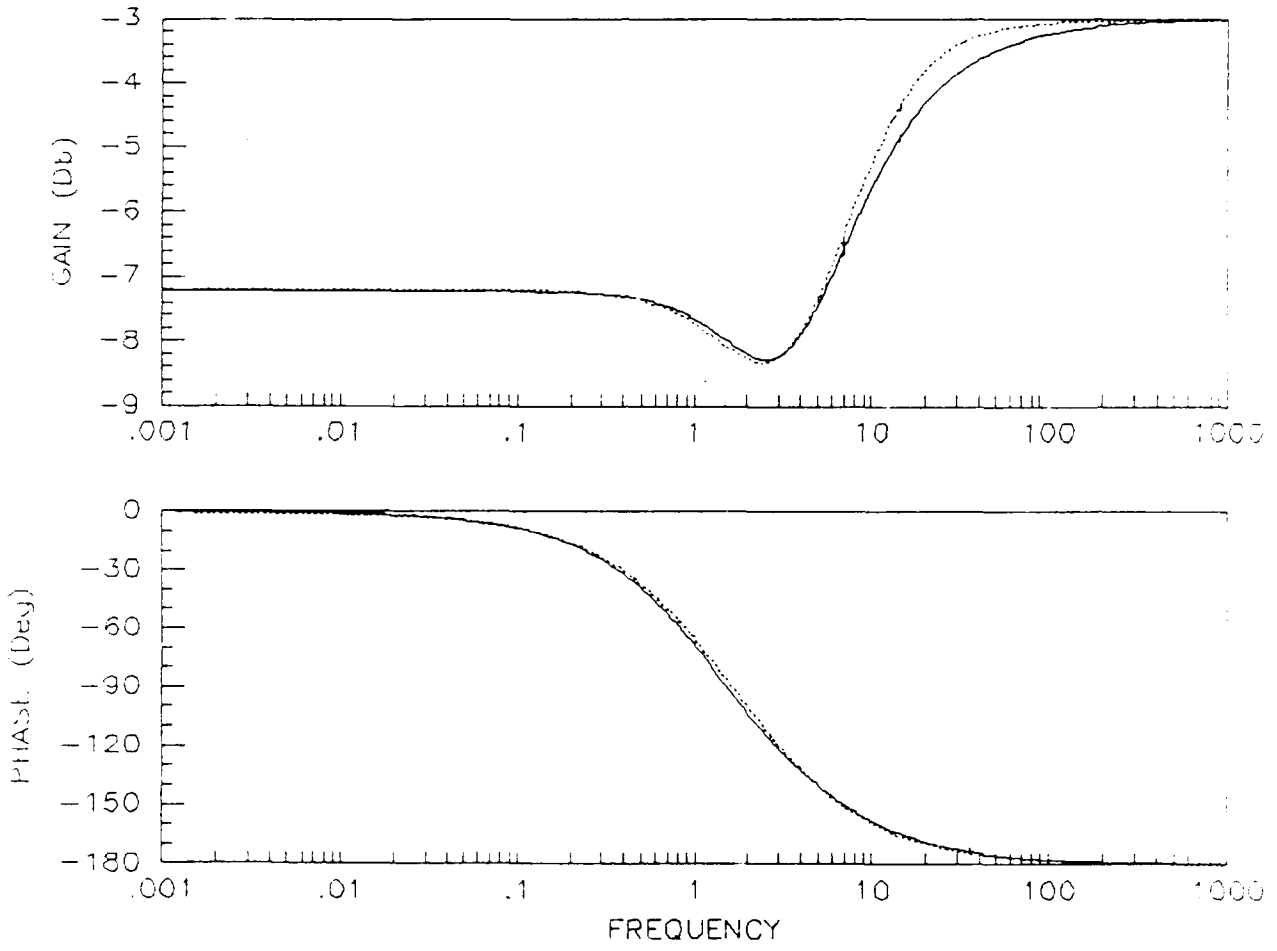

Figure 2.5. Plot of $\mathbf{u_{22}}(j\omega)$

to describe $\sigma_1(\omega)$ and $\sigma_2(\omega)$. As such, any description of the $\sigma_i(\omega)$ plots is accomplished either by seperately describing the magnitude and phase of the function, or by using functions which are not real-rational.

The continuous lines of Figures 2.2 through 2.5 are plots of the transfer function elements $\mathbf{u_{ij}(j\omega)}$, $i = 1, 2$, $j = 1, 2$, of $\mathbf{U(j\omega)}$. Note that $\mathbf{u_{11}(j\omega)}$ and $\mathbf{u_{12}(j\omega)}$ cannot be described as real rational functions of $j\omega$. From (3:268), the phase difference at $\omega = \infty$ is $90^\circ \times (n - w)$, where $(n - w)$ is the difference in the orders of the denominator and numerator polynomials of a transfer function. For the given plots, the phase plots of u_{11} and of u_{12} indicate that $(n - w)$ is odd. However, the zero slopes for each of these plots as $\omega \rightarrow \infty$ indicate that the difference in the orders of the polynomials is zero. Hence, any description of the $\mathbf{u_{11}(j\omega)}$ and $\mathbf{u_{12}(j\omega)}$ must again be made either by separately describing the magnitude and phase of the function, or by separately describing the real and imaginary parts of the function. There can be no real rational function in $j\omega$ to describe the first column entries of $\mathbf{U(j\omega)}$.

Having commented on the existence of functions needed to describe $\mathbf{\Sigma}(\omega)$ and $\mathbf{U(j\omega)}$, a curve fitting approximation is obtained for each of the provided plots. Using $|\mathbf{U}(\omega)|$ to indicate the magnitude of the function, and $\angle\mathbf{U}(\omega)$ to indicate the phase, the elements of $\mathbf{\Sigma}(\omega)$ and $\mathbf{U(j\omega)}$ are approximated to be as follows. Elements of $\mathbf{V^*(j\omega)}$ (if desired) are similarly obtained.

$$\mathbf{\Sigma}(\omega) = \begin{pmatrix} \left[\frac{0.994}{\omega^2+0.994}\right]^{\frac{1}{2}} & 0 & 0 \\ 0 & \left[\frac{0.994}{\omega^2+28.09}\right]^{\frac{1}{2}} & 0 \end{pmatrix}$$

$$|\mathbf{U(j\omega)}| = \begin{pmatrix} \left|\frac{0.702(j\omega+2.71)(j\omega+3.75)}{(j\omega+1.67)(j\omega+9.8)}\right| & \left|\frac{0.711(j\omega+1)(j\omega+17)}{(j\omega+1.044)(j\omega+12.9)}\right| \\ \left|\frac{0.711(j\omega+1)(j\omega+17)}{(j\omega+1.044)(j\omega+12.9)}\right| & \left|\frac{0.702(j\omega+2.71)(j\omega+3.75)}{(j\omega+1.67)(j\omega+9.8)}\right| \end{pmatrix}$$

$$\angle \mathbf{U}(\mathbf{j}\omega) = \begin{pmatrix} \angle \frac{-1}{(j\omega+2)^3} & \angle \frac{-1}{(j\omega+2)^3} \\ \angle \frac{-1}{(j\omega+1)(j\omega+2.75)} & \angle \frac{1}{(j\omega+1)(j\omega+2.75)} \end{pmatrix}$$

The dotted lines of Figures 2.1 through 2.5 result from the determined approximations. In Figure 2.1, the dotted lines overlap the continuous (actual) functions quite well. If $\mathbf{U}^*(\mathbf{j}\omega)$ is required, it is obtainable as $\mathbf{U}^*(\mathbf{j}\omega) = |\mathbf{U}(\mathbf{j}\omega)|^{-1} \angle \mathbf{U}(\mathbf{j}\omega)$.

Before closing this section, two final notes are made. First, the elements of the $\mathbf{\Sigma}(\omega)$ and $\mathbf{U}(\mathbf{j}\omega)$ are approximations. It is generally impossible to find a real-rational functions in $j\omega$ that produce the curves obtained for elements of the $\mathbf{U}(\mathbf{j}\omega)$, $\mathbf{\Sigma}(\omega)$, and $\mathbf{V}(\mathbf{j}\omega)$ matrices.

Second, the functions used in the test example are simple, well-behaved functions. There is no occurrence of a singular value crossing. If a crossing had occurred, discontinuous descriptions of functions may have been necessary. However since the process of curve fitting is imperfect, function discontinuities may actually go unnoticed in obtaining a workable singular value decomposition.

Hence, approximations to the singular value decomposition of a matrix of transfer functions $\mathbf{P}(\mathbf{j}\omega)$ are obtainable. However, because of inherent difficulties in obtaining acceptable curve fitting approximations to polynomials of higher order than are used in the example $\mathbf{P}(\mathbf{j}\omega)$, the use of the singular value decomposition for obtaining solutions to the model-matching problem is limited.

2.5 *Spectral Relationships Using Singular Values*

Assume σ is a singular value function of a matrix P, that $\mathbf{P}(\mathbf{j}\omega)$ is the Fourier transform of $P(t)$ and that $\mathbf{P}(\mathbf{j}\omega)$ is obtainable from $P(t)$. [2]

[2]The term P is used in this section to indicate that either $P(t)$, or $\mathbf{P}(\mathbf{j}\omega)$ is in use; when there is a need to differentiate, clarification is made.

The function defining the singular values σ_i of P as the positive square root of the eigenvalues λ of P^*P is given by

$$\sigma_i(P) = \lambda_i^{\frac{1}{2}}(P^*P) \tag{2.12}$$

where λ satisfies the determinant (det) equation

$$det(\lambda I - P^*P) = 0 \tag{2.13}$$

Let $A = P^*P$. Then for $A = [a_{ij}]^{m\times m}$ and P assumed to be $l \times m$, Equation (2.13) is expanded to yield

$$\begin{pmatrix} (\lambda - a_{11}) & + & a_{12} & + & \dots & + & a_{1m} \\ a_{21} & + & (\lambda - a_{22}) & + & \dots & + & a_{2m} \\ \vdots & & \vdots & & & \vdots & \\ a_{m1} & + & a_{m2} & + & \dots & + & (\lambda - a_{\dots m}) \end{pmatrix} = 0_{m\times m}$$

From the above set of equations, the characteristic equation of A is determined. The characteristic equation is given by

$$\lambda^m + k_1\lambda^{(m-1)} + \dots + k_{m-1}\lambda + k_m = 0 \tag{2.14}$$

Written in factored form, Equation (2.14) becomes

$$(\lambda - \lambda_1)(\lambda - \lambda_2)\dots(\lambda - \lambda_{m-1})(\lambda - \lambda_m) = 0 \tag{2.15}$$

The following is known concerning the sums and products of the λ_i eigenvalues of any square matrix A (2:208-209):

$$\sum_{i=1}^{m} \lambda_i = trace(A) \tag{2.16}$$

$$\prod_{i=1}^{m} \lambda_i = k_m \tag{2.17}$$

The product of two matrices M_1 and M_2, $M_1 = [\alpha_{ij}]^{n \times m}$ and $M_2 = [\beta_{ij}]^{m \times q}$, is defined by

$$[\alpha_{ij}]^{n \times m} \cdot [\beta_{ij}]^{m \times q} = [\gamma_{ij}]^{n \times q} \tag{2.18}$$

where

$$\sum_{k=1}^{m} \alpha_{ik} \beta_{kj} = \gamma_{ij};\ i = 1, 2, \ldots n,\ j = 1, 2, \ldots q \tag{2.19}$$

For $A = P^* P$, $P = [p_{ij}]^{q \times n}$ and $P^* = [\overline{p}_{ji}]^{n \times q}$, Equation (2.19) yields

$$\gamma_{ij} = \sum_{k=1}^{q} \overline{p}_{ki} p_{kj};\ i, j = 1, 2, \ldots n \tag{2.20}$$

To obtain elements of the $trace(A) = trace(P^*P)$, set $i = j$ and obtain

$$\gamma_{ii} = \sum_{k=1}^{q} \overline{p}_{ki} p_{ki} \quad i = 1, 2, ..., n \tag{2.21}$$

so that $trace(A) = trace(P^*P)$ is given by

$$trace(A) = \sum_{i=1}^{n} \gamma_{ii} = \sum_{i=1}^{n} \sum_{k=1}^{q} \overline{p}_{ki} p_{ki} \tag{2.22}$$

Equations (2.16) and (2.22) are combined to yield

$$\sum_{i=1}^{n} \lambda_i = \sum_{i=1}^{n} \sum_{k=1}^{q} \overline{p}_{ki} p_{ki} \tag{2.23}$$

Hence, if the p_{ki} are replaced by their Fourier transforms, it can be concluded that the sum of the squared singular values of $\mathbf{P}(\mathbf{j}\omega)$ (the matrix whose elements are the $\mathbf{p_{ki}}(\mathbf{j}\omega)$) evaluated at any frequency equals the system's total spectral energy density function (the sum of the $\overline{\mathbf{p}}_{\mathbf{ki}}(\mathbf{j}\omega)\mathbf{p_{ki}}(\mathbf{j}\omega)$ evaluated at the same frequency).

Integrating Equation (2.23), and comparing it to Equation (2.3) indicates that the total energy E in a system is given by

$$\begin{aligned} E &= \frac{1}{2\pi} \int_{-\infty}^{\infty} \sum_{i=1}^{n} \sum_{k=1}^{q} p_{ki}^2(t) dt \\ &= \frac{1}{2\pi} \int_{-\infty}^{\infty} \sum_{i=1}^{n} \lambda_i(t) dt \end{aligned} \tag{2.24}$$

$$= \frac{1}{2\pi}\int_{-\infty}^{\infty} trace(A(t))dt \tag{2.25}$$

For functions in the frequency domain, E is given by [3]

$$\begin{aligned} E &= \frac{1}{2\pi}\int_{-\infty}^{\infty}\sum_{i=1}^{n}\sum_{k=1}^{q}\bar{\mathbf{p}}_{\mathbf{ki}}(\mathrm{j}\omega)\mathbf{p}_{\mathbf{ki}}(\mathrm{j}\omega)d\omega \\ &= \frac{1}{2\pi}\int_{-\infty}^{\infty}\sum_{i=1}^{n}\lambda_{\mathbf{i}}(\mathrm{j}\omega)d\omega \end{aligned} \tag{2.26}$$

2.6 *Spectral Relationships to Norm Minimization*

To begin this section, the Hardy spaces known as H_2 and H_∞ are defined.

The H_2 space consists of all compex-valued functions $\mathbf{P}(\mathrm{j}\omega)$ that are analytic in the open right half plane and that satisfy the following condition

$$\left(\frac{1}{2\pi}\int_{-\infty}^{\infty} trace[\mathbf{P}^*(\mathrm{j}\omega)\mathbf{P}^*(\mathrm{j}\omega)]d\omega\right)^{\frac{1}{2}} < \infty \tag{2.27}$$

The left hand side of the inequality is defined to be the H_2-norm of $\mathbf{P}(\mathrm{j}\omega)$, and is denoted as $\|\mathbf{P}(\mathrm{j}\omega)\|_2$.

Alternately, H_∞ consists of all complex-valued functions $\mathbf{P}(\mathrm{j}\omega)$ which are analytic and bounded in the open right half plane. By bounded, it is meant that there exists a real number b such that

[3] Eigenvalues of P^*P equal the singular values of P^*P (proof given later). Hence, the $\lambda_{\mathbf{i}}(\mathrm{j}\omega)$ in Equation (2.26) are nonnegative functions of $j\omega$.

$$\sigma_{max}[\mathbf{P}(\mathrm{j}\omega)] \leq b \tag{2.28}$$

where σ_{max} represents the largest singular value of $\mathbf{P}(\mathrm{j}\omega)$. The least such bound b is the H_∞-norm of $\mathbf{P}(\mathrm{j}\omega)$, denoted $\|\mathbf{P}(\mathrm{j}\omega)\|_\infty$. Equivalently

$$\|\mathbf{P}(\mathrm{j}\omega)\|_\infty = \sup_\omega \sigma_{max}[\mathbf{P}(\mathrm{j}\omega)] \tag{2.29}$$

where sup over ω is the supremum of the maximum singular value σ_{max} of $\mathbf{P}(\mathrm{j}\omega)$ over all frequencies.

Relationships between the H_2 and H_∞-norms and the power and spectral densities are now defined. Equations (2.26) and (2.27) are combined to obtain

$$\begin{aligned} \|\mathbf{P}(\mathrm{j}\omega)\|_2 &= \left(\frac{1}{2\pi}\int_{-\infty}^{\infty}\sum_{i=1}^{n}\sum_{k=1}^{q}\overline{\mathrm{Pki}}(\mathrm{j}\omega)\mathrm{Pki}(\mathrm{j}\omega)\mathrm{d}\omega\right)^{\frac{1}{2}} \\ &= \left(\frac{1}{2\pi}\int_{-\infty}^{\infty}\sum_{i=1}^{n}\lambda_{\mathrm{i}}(\mathrm{j}\omega)d\omega\right)^{\frac{1}{2}} \\ &= \sqrt{E} \end{aligned} \tag{2.30}$$

Hence, for any signal $\mathbf{v}(\mathrm{j}\omega)$, the H_2-norm of $\mathbf{v}(\mathrm{j}\omega)$ is interpretable as the square root of the energy of the signal. This fact is noted by Francis (5:6). That the H_2-norm is also related to the *trace* of the power spectrum is obvious after substituting Equation (2.12) into Equation (2.29).

Now the standard model-matching problem is considered. The objective of

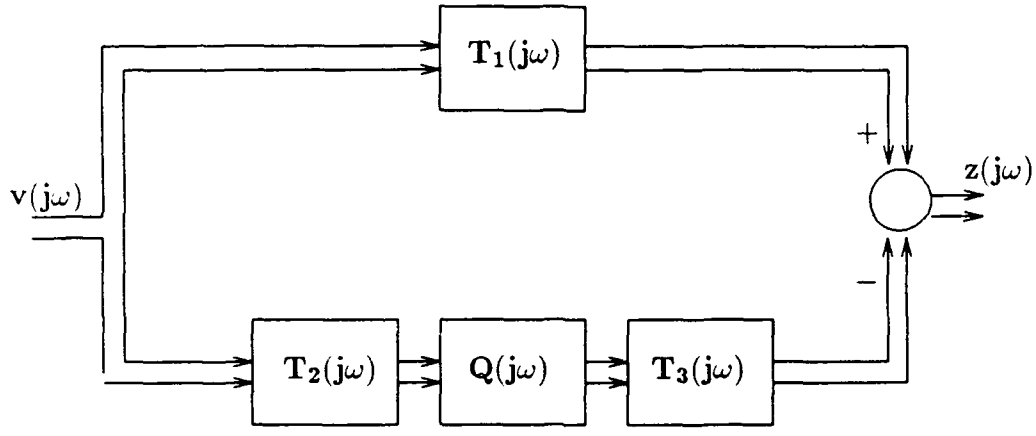

Figure 2.6. Model-Matching Problem

model-matching is to minimize $\|\mathbf{\Phi}(j\omega)\|$ where $\|\mathbf{\Phi}(j\omega)\| = \|\mathbf{T_1}(j\omega) - \mathbf{T_2}(j\omega)\mathbf{Q}(j\omega\mathbf{T_3}(j\omega)\|$, $\mathbf{T_i}(\omega)$ fixed and $\mathbf{Q}(j\omega)$ unknown (see Figure 2.6) . By comparing the model-matching problem with Equation (2.30), it is concluded that H_2-norm minimization minimizes the total energy of $\mathbf{\Phi}(j\omega)$. A similar relationship exists for the H_∞-norm.

Squaring both sides of Equation (2.29) and letting σ^2_{max} denote the square of the maximum singular, equations (2.12) and (2.29) are applied to obtain the following series of equalities.

$$\begin{aligned}
\|\mathbf{P}(j\omega)\|^2_\infty &= (\sup_\omega \sigma_{max}[\mathbf{P}(j\omega)])^2 \\
&= \sup_\omega \sigma^2_{max}[\mathbf{P}(j\omega)] \\
&= \sup_\omega \lambda_{max}[\mathbf{P}^*(j\omega)\mathbf{P}(j\omega)] \\
&= \sup_\omega \lambda^{\frac{1}{2}}_{max}[\mathbf{P}^*(j\omega)\mathbf{P}(j\omega)]^*[\mathbf{P}^*(j\omega)\mathbf{P}(j\omega)] \\
&= \sup_\omega \sigma_{max}[\mathbf{P}^*(j\omega)\mathbf{P}(j\omega)] \qquad (2.31)
\end{aligned}$$

In addition, based upon equalities between intermediate steps in Equation (2.31), it is also concluded that

$$\sup_{\omega} \sigma_{max} [\mathbf{P}^*(j\omega)\mathbf{P}(j\omega)] = \sup_{\omega} \lambda_{max} [\mathbf{P}^*(j\omega)\mathbf{P}(j\omega)] \tag{2.32}$$

Equation (2.32) indicates that the singular values of any Hermetian matrix $A = [\mathbf{P}^*(j\omega)\mathbf{P}(j\omega)]$ equal the eigenvalues of A. As such, the eigenvalues of $[\mathbf{P}^*(j\omega)\mathbf{P}(j\omega)]$ are nonnegative.

Next, the product of a unitary matrix $\mathbf{U}(j\omega)$ and a matrix $\mathbf{P}(j\omega)$ is formed. The H_∞-norm of the product is given by

$$\begin{aligned}
\|\mathbf{U}(j\omega)\,\mathbf{P}(j\omega)\|_\infty &= \sup_{\omega} \sigma_{max} [\mathbf{U}(j\omega)\,\mathbf{P}(j\omega)] \\
&= \sup_{\omega} \lambda_{max}^{\frac{1}{2}} [\mathbf{U}(j\omega)\,\mathbf{P}(j\omega)]^* [\mathbf{U}(j\omega)\,\mathbf{P}(j\omega)] \\
&= \sup_{\omega} \lambda_{max}^{\frac{1}{2}} [\mathbf{P}^*(j\omega)\,\mathbf{U}^*(j\omega)\mathbf{U}(j\omega)\,\mathbf{P}(j\omega)] \\
&= \sup_{\omega} \lambda_{max}^{\frac{1}{2}} [\mathbf{P}^*(j\omega)\mathbf{P}(j\omega)] \\
&= \|\mathbf{P}(j\omega)\|_\infty
\end{aligned}$$

Similarly, it can be shown that $\|\mathbf{P}(j\omega)\mathbf{U}(j\omega)\|_\infty = \|\mathbf{P}(j\omega)\|_\infty$.

As a result, it is concluded that the H_∞-norm of matrices formed by the pre- or post-multiplication of any matrix $\mathbf{P}(j\omega)$ by unitary matrices is the H_∞-norm of $\mathbf{P}(j\omega)$ alone.

A parallel result concerning the H_2-norm of unitary matrices can also be shown. That is,

$$
\begin{aligned}
\|\mathbf{U}(j\omega)\,\mathbf{P}(j\omega)\|_2 &= \left(\frac{1}{2\pi}\int_{-\infty}^{\infty} trace[[\mathbf{U}(j\omega)\mathbf{P}(j\omega)]^*\,[\mathbf{U}(j\omega)\mathbf{P}(j\omega)]]d\omega\right)^{\frac{1}{2}} \\
&= \left(\frac{1}{2\pi}\int_{-\infty}^{\infty} trace[\mathbf{P}^*(j\omega)\mathbf{U}^*(j\omega)\,\mathbf{U}(j\omega)\mathbf{P}(j\omega)]d\omega\right)^{\frac{1}{2}} \\
&= \left(\frac{1}{2\pi}\int_{-\infty}^{\infty} trace[\mathbf{P}^*(j\omega)\,\mathbf{P}(j\omega)]d\omega\right)^{\frac{1}{2}} \\
&= \|\mathbf{P}(j\omega)\|_2
\end{aligned}
$$

and,

$$
\begin{aligned}
\|\mathbf{P}(j\omega)\,\mathbf{U}(j\omega)\|_2 &= \left(\frac{1}{2\pi}\int_{-\infty}^{\infty} trace[[\mathbf{P}(j\omega)\mathbf{U}(j\omega)]^*\,[\mathbf{P}(j\omega)\mathbf{U}(j\omega)]]d\omega\right)^{\frac{1}{2}} \\
&= \left(\frac{1}{2\pi}\int_{-\infty}^{\infty} trace[[\mathbf{P}(j\omega)\mathbf{U}(j\omega)]\,[\mathbf{P}(j\omega)\mathbf{U}(j\omega)]^*]d\omega\right)^{\frac{1}{2}} \\
&= \|\mathbf{P}(j\omega)\|_2
\end{aligned}
$$

where the fact that $trace(AB) = trace(BA)$ is used. Thus unitary matrices are both H_2 and H_∞-norm invariant. Multiplying any matrix by a unitary matrix does not change either its H_2 or H_∞-norm. In addition, it is also concluded that inherent differences between energy and power signals makes the choice of whether to use H_2 or H_∞-norm minimization criteria application dependent.

2.7 *Boundaries on Model Matching Problem Solutions*

A sufficient condition for the existence of a solution to the model matching problem is provided by Theorem 1.1 (5). The theorem states that an optimal $\mathbf{Q}(j\omega)$ to the model matching problem exists if the ranks of the $\mathbf{T_2}(j\omega)$ and $\mathbf{T_3}(j\omega)$ are

constant for all $0 < \omega \leq \infty$.

Now again consider Equation (2.1), the minimization equation using the H_2 or H_∞-norm. As both the H_2 and the H_∞-norm are normed spaces, they satisfy the Schwartz-inequality and hence

$$\|\mathbf{\Phi}(j\omega)\|_{2,\infty} = \|\mathbf{T_1}(j\omega) - \mathbf{T_2}(j\omega)\mathbf{Q}(j\omega)\mathbf{T_3}(j\omega)\|_{2,\infty} \tag{2.33}$$

implies that

$$\|\mathbf{\Phi}(j\omega)\|_{2,\infty} \leq \|\mathbf{T_1}(j\omega)\|_{2,\infty} + \|\mathbf{T_2}(j\omega)\mathbf{Q}(j\omega)\mathbf{T_3}(j\omega)\|_{2,\infty} \tag{2.34}$$

Using the above equation and inequality, we are able to define both a lower and an upper bound for model matching problem solutions. The lower bound is given when $\mathbf{T_1}(j\omega) = [\mathbf{T_2}(j\omega)\mathbf{Q}(j\omega)\mathbf{T_3}(j\omega)]$ in which case $\|\mathbf{\Phi}(j\omega)\|_{2,\infty} = 0$.

The upper bound is given by setting $\mathbf{Q}(j\omega) = 0$ in which case $\|\mathbf{\Phi}(j\omega)\|_\infty = \|\mathbf{T_1}(j\omega)\|_{2,\infty}$. Hence, if a solution exists, then the optimal solution can be sought via an iterative process on selections of $\mathbf{Q}(j\omega) \in RH_\infty$, since the following inequality is always satisfied

$$0 \leq \mathbf{\Phi}(j\omega)\|_{2,\infty} \leq \|\mathbf{T_1}(j\omega)\|_{2,\infty} \tag{2.35}$$

The Quantitative Feedback Technique is now examined before relating QFT to the use of H_2 and H_∞ minimization.

2.8 *The Quantitative Feedback Technique*

Figure 2.7 represents an $l \times l$ MIMO closed-loop system in which $\mathbf{F}(j\omega)$ is the matrix of prefilter transfer functions, $\mathbf{G}(j\omega)$ is the matrix of compensating transfer functions, and $\mathbf{P_e}(j\omega) = \mathbf{P}(j\omega)\mathbf{Q}(j\omega)$. Note that the feedback matrix is set to I, since an equivalent cascade compensator with prefilter is determinable for any nonunity expression that could be used here.

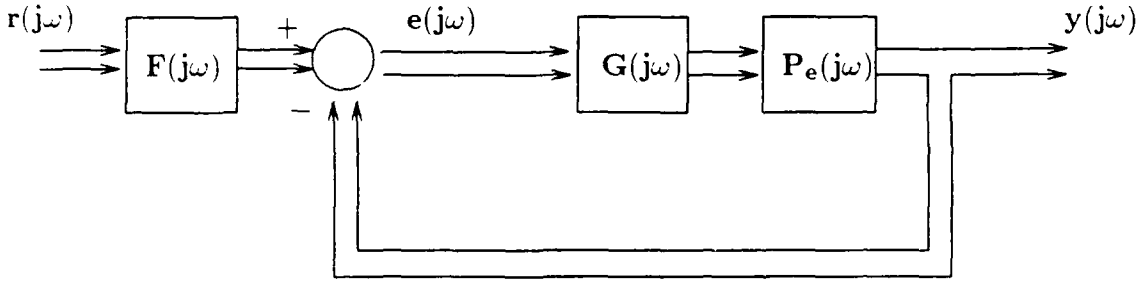

Figure 2.7. The QFT Compensated Equivalent Plant

When performing a QFT design, the compensator $\mathbf{G}(j\omega)$ is typically assumed diagonal. The use of nondiagonal $\mathbf{G}(j\omega)$ matrices has been used in the past to give designers more flexibility in their designs (3:698). However, the use of nondiagonal $\mathbf{G}(j\omega)$ increases the work associated with determining $\mathbf{G}(j\omega)$.

From Figure 2.7, the following equations can be written:

$$\mathbf{y}(j\omega) = \mathbf{P_e}(j\omega)\mathbf{G}(j\omega)\mathbf{e}(j\omega) \tag{2.36}$$

$$\mathbf{e}(j\omega) = \mathbf{F}(j\omega)\mathbf{r}(j\omega) - \mathbf{y}(j\omega) \tag{2.37}$$

$$\mathbf{y}(j\omega) = [I + \mathbf{P_e}(j\omega)\mathbf{G}(j\omega)]^{-1}\mathbf{P_e}(j\omega)\mathbf{G}(j\omega)\mathbf{F}(j\omega)\mathbf{r}(j\omega) \tag{2.38}$$

Equation (2.38) above gives the MIMO system control ratio $\mathbf{T}(j\omega)$ relating $\mathbf{r}(j\omega)$ to $\mathbf{y}(j\omega)$ as

$$\mathbf{T}(j\omega) = [I + \mathbf{P_e}(j\omega)\mathbf{G}(j\omega)]^{-1}\mathbf{P_e}(j\omega)\mathbf{G}(j\omega)\mathbf{F}(j\omega) \tag{2.39}$$

The QFT design procedure requires finding the unknown transfer function elements of $\mathbf{G}(j\omega)$ and $\mathbf{F}(j\omega)$, by using performance specifications to define tolerance bounds on the transfer function elements of $[I + \mathbf{P_e}(j\omega)\mathbf{G}(j\omega)]^{-1}\mathbf{P_e}(j\omega)\mathbf{G}(j\omega)\mathbf{F}(j\omega)$. To do so, a mapping between a MIMO plant and a set of equivalent multiple-input, single-output (MISO) control systems is defined. The mapping results in l^2 equivalent systems for a MIMO plant $\mathbf{P_e}(j\omega)$ assumed to be $l \times l$, with each transfer function of the equivalent MISO system assumed to have two inputs and one output. Of the two inputs, one is designated the desirable input, while the other is designated the "disturbance" input (3:696–699).

The justification of the MISO equivalent method follows (7) and (3). The inverse of a square, (assumed invertible) plant matrix is represented by

$$P_e^{-1} = \begin{pmatrix} m_{11} & m_{12} & \dots & m_{1m} \\ m_{21} & m_{22} & \dots & m_{2m} \\ \vdots & \vdots & & \vdots \\ m_{m1} & m_{m2} & \dots & m_{mm} \end{pmatrix}$$

where the m_{ij} are elements of the adjoint of P_e, divided by $det(P_e)$. The $l \times l$ MISO equivalent plant is the matrix formed by inverting individual elements of $\mathbf{P_e^{-1}}(j\omega)$ so that each v_{ij} element of V satisfies $v_{ij} = (m_{ij})^{-1}$. The MISO equivalent matrix is given by

$$V = \begin{pmatrix} (m_{11})^{-1} & (m_{12})^{-1} & \dots & (m_{1m})^{-1} \\ (m_{21})^{-1} & (m_{22})^{-1} & \dots & (m_{2m})^{-1} \\ \vdots & \vdots & & \vdots \\ (m_{m1})^{-1} & (m_{m2})^{-1} & \dots & (m_{mm})^{-1} \end{pmatrix} = \begin{pmatrix} v_{11} & v_{12} & \dots & v_{1m} \\ v_{21} & v_{22} & \dots & v_{2m} \\ \vdots & \vdots & & \vdots \\ v_{m1} & v_{m2} & \dots & v_{mm} \end{pmatrix}$$

The matrix $\mathbf{P_e^{-1}}(j\omega)$ is next partitioned into two parts; the first part $\mathbf{D}(j\omega)$ contains the diagonal elements of $\mathbf{P_e^{-1}}(j\omega)$ and the second part $\mathbf{B}(j\omega)$ contains the balance of $\mathbf{P_e^{-1}}(j\omega)$. That is

$$\begin{aligned} \mathbf{P_e^{-1}}(j\omega) &= \mathbf{D}(j\omega) + \mathbf{B}(j\omega) \\ &= [m_{ij}] \\ &= [\frac{1}{v_{ij}}] \end{aligned} \qquad (2.40)$$

Both sides of Equation (2.40) are next premultiplied by $[I + \mathbf{P_e}(j\omega)\mathbf{G}(j\omega)]$, to obtain

$$[I + \mathbf{P_e}(j\omega)\mathbf{G}(j\omega)]\mathbf{T}(j\omega) = \mathbf{P_e}(j\omega)\mathbf{G}(j\omega)\mathbf{F}(j\omega) \qquad (2.41)$$

Next, both sides of Equation (2.41) are premultiplied by $\mathbf{P_e^{-1}}(j\omega)$ (assumed invertible), to obtain

$$[\mathbf{P_e^{-1}}(\omega) + \mathbf{G}(j\omega)]\mathbf{T}(j\omega) = \mathbf{G}(j\omega)\mathbf{F}(j\omega) \tag{2.42}$$

The equality $\mathbf{P_e^{-1}}(j\omega) = \mathbf{D}(j\omega) + \mathbf{B}(j\omega)$ is now substituted into Equation (2.42) to yield

$$[[\mathbf{D}(j\omega) + \mathbf{B}(j\omega)] + \mathbf{G}(j\omega)]\mathbf{T}(j\omega) = \mathbf{G}(j\omega)\mathbf{F}(j\omega) \tag{2.43}$$

Multiply out the terms on the left side of the equation. Subtract $\mathbf{B}(j\omega)\mathbf{T}(j\omega)$ from both sides and then premultiply by $[\mathbf{D}(j\omega) + \mathbf{G}(j\omega)]^{-1}$, which is invertible for $\mathbf{G}(j\omega)$ assumed to be diagonal. Thus

$$\mathbf{T}(j\omega) = [\mathbf{D}(j\omega) + \mathbf{G}(j\omega)]^{-1}[\mathbf{G}(j\omega)\mathbf{F}(j\omega) - \mathbf{B}(j\omega)\mathbf{T}(j\omega)] \tag{2.44}$$

This last equation is used to define the desired mapping. The proof of the fact that designs based on MISO equivalent systems yield satisfactory MIMO designs for the original plant is based on Schauder's fixed point theorem. The theorem is invoked by defining a mapping $Y(T) = [D + G]^{-1}[GF - BT]$ where each member of T is from an acceptable set of control ratios satisfying the design requirements (3:699-700).

Individual elements of $[D+G]^{-1}$ are scalars multiplying rows of $[GF-BT]$, with

$$\begin{aligned}[d_{ii}+g_{ii}]^{-1} &= [\frac{1}{v_{ii}}+g_{ii}]^{-1} \\ &= \frac{v_{ii}}{1+v_{ii}g_{ii}} \end{aligned} \tag{2.45}$$

For a unit impulse forcing function, the y_{ij} elements of the mapping $Y(T)$ take on the form

$$\begin{aligned} y_{ij} &= \frac{d_{ii}}{1+d_{ii}g_{ii}}[g_{ii}f_{ij}-\sum_{k\neq i} b_{ij}t_{ij}] \\ &= \frac{v_{ii}}{1+v_{ii}g_{ii}}[g_{ii}f_{ij}-\sum_{k\neq i} v_{ij}t_{ij}] \end{aligned} \tag{2.46}$$

Equation (2.46) is also the control ratio of the i^{th} MISO system. The transfer function given by

$$\frac{v_{ii}}{1+v_{ii}g_{ii}}[g_{ii}f_{ij}] \tag{2.47}$$

represents the "desired" i^{th} output with respect to the desired j^{th} input while the transfer function

$$\frac{v_{ii}}{1 + v_{ii}g_{ii}}[\sum_{k \neq i} v_{ij}t_{ij}] \tag{2.48}$$

relates the i^{th} output to the j^{th} "disturbance" input. The objective of the design is then to have each loop track the desired input while minimizing the outputs due to the disturbance inputs.

For plants that are basically noninteracting (BNIC) (i.e., highly diagonally dominant), the magnitude of functions represented by Equation (2.48) is small relative to those represented by Equation (2.47). For such systems, QFT designs can be pursued using diagonal $\mathbf{F}(\mathbf{j}\omega)$ prefilters.

For disturbance-rejection problems, the y_{ij} responses are designed to be less than some bound k; the boundary value with respect to the i^{th} input and the j^{th} output, k_{ij}, is then used to obtain the desired MIMO design by obtaining transfer functions that satify $k_{ij} \geq |\frac{v_{ii}}{1+v_{ii}g_{ii}}|[\sum_{k \neq i} v_{ij}t_{ij}]$. Solutions are obtained by reorganizing the inequality into a form that yields the loop transfer function, and then following the QFT process given in (7).

It has been shown that a realistic definition of optimum for purposes of QFT designs on LTI systems is the minimization of the high-frequency loop gain. It has also been proven that this optimum lies on the composite boundary formed by determining the maximum of two error sources: plant deviations due to disturbance inputs and tracking errors. It has also been proven that the optimum is unique (7:2-26). The optimal design is, however, not achievable. Instead, designs that yield responses that are relatively close to the composite boundary without crossing it are deemed acceptable, although they encompass some amount of overdesign.

The QFT process is simplified if the m_{ij} of P_e^{-1} are MP. This is, however, not a QFT requirement, since the $v_{ij} = (m_{ij})^{-1}$ need not be stable for development of a QFT design.

However, since poles of the m_{ij} of P_e^{-1} appear as zeros of the v_{ij} functions used in the QFT design, the use of QFT in its simplest form requires that all poles of the m_{ij} be in the LHP. Hence, it is important to consider the impact of not having all LHP zeros on a QFT design before proceeding further.

2.8.1 The Impact of NMP v_{ij} on QFT Designs A v_{ij} transfer function of a MISO equivalent plant is NMP if a zero of the transfer function lies in the RHP. Systems with RHP zeros cause considerable difficulty in control designs; the zeros have a marked influence on the nature of a system's time response. Whenever there is a RHP zero, the initial time response of the plant is negative, even though the steady state value is positive. In addition, branches of the root loci that start at open-loop poles must end at the zeros or ∞. For any simple feedback system that may be implemented, the closed-loop poles lie somewhere on the root locus between a starting pole and either an ending zero or ∞. The location of the closed-loop poles depends on the selected value of feedback gain. As the selected value of gain is increased, poles of the closed-loop system approach the $j\omega$- axis. If the gain is selected large enough, closed-loop poles in the RHP are obtained, and the closed-loop system becomes unstable.

For NMP v_{ij}, tolerances on both the phase and the magnitude of the tracking response must be specified; for MP v_{ij}, only the magnitude of the tracking response is specified. While it is considerably easier to work with MP systems, it is not an absolute requirement in order to perform a QFT design (3:692). QFT designs are typically pursued only for MP systems, since it is for such systems that QFT guarantees a solution meeting stated performance objectives for the entire set of possible plants (assuming tolerances have not been too tightly specified).

The occurence of NMP behavior is a function of where actuators and sensors are mounted. System zero locations are changed if the location of the actuator and sensor devices is changed. Hence, the NMP nature of a v_{ij} can be addressed as a need

to alter the systems's configuration by relocating control devices. However, once the location of a set of actuator and sensor devices is decided upon, any NMP behavior and inherent control design difficulties that result must be dealt with accordingly (15:2-36).

2.8.2 Methods for Determining if a Matrix is NMP The current literature offers a number of ways to determine if any v_{ij} are MP. Three methods are examined.

2.8.2.1 Routh's Stability Criterion Routh's criterion is a simple method for determining the presence of RHP roots without actually solving for the roots. The criterion states that the number of roots of the polynominal with positive real parts is equal to the number of sign changes of array coefficients in the first column (3:185–191).

While Routh's criterion is primarily used for determining system stability, it can be used to determine if any v_{ij} have zeros in the RHP by applying the criterion to the denominator polynomial of $det(\mathbf{P_e}(j\omega))$. The application of Routh's criterion is straightforward, when $\mathbf{Q}(j\omega)$ is known and $\mathbf{P}(j\omega)$ is fixed. However, if the plant varies, and if $\mathbf{Q}(j\omega)$ is unknown, then the application of Routh's criterion becomes increasingly difficult.

2.8.2.2 Evaluation Based on Step Response The author of (20) offers a simple necessary and sufficient condition for a stable SISO plant to exhibit an undershooting step response. Specifically, the author shows that undershoot occurs if and only if the transfer function of a stable SISO plant has an odd number of real RHP zeros.

Consider a system with a strictly proper, real-rational transfer function $p(j\omega)$. Further, suppose the system is stable and has a steady state value not equal to zero. Let $y(t)$ denote the time response of the system in response to a step input. Then for an assumed stable system, $y(\infty)$ is well-defined and equals $p(j\omega)$ evaluated at

$\omega = 0$.

The author show that undershoot in stable systems in response to a step input occurs only if the steady-state value has a sign opposite from that of its first nonzero derivative. To define when undershoot occurs first requires defining the relative order of a polynomial. The relative order of a transfer function, denoted as r, is the difference between the orders of the numerator and denominator polynomials of the function. In (20), a plant is shown to exhibit undershoot only if the product of the r^{th} derivative and the steady state value, $y^r(0)\, y(\infty)$ is less than zero.

The evaluation method described in (20) can be used to evaluate the v_{ij}, but the method is more involved than evaluations using other methods. As such, it is unlikely that this method can be incorporated into design processes involving the selection of a suitable $\mathbf{Q}(\mathrm{j}\omega)$.

2.8.2.3 *Evaluation of a Composite Matrix* The authors of (14) offer a necessary and sufficient condition for the stability of a polynomial matrix. Changes in the presentation as made by the authors of (14) are made herein to make the material suitable to this section.

Define $\mathbf{P}'_{\mathbf{e}}(\mathrm{j}\omega)$ as that polynomial matrix resulting from the product of $\mathbf{P_e}(\mathrm{j}\omega)$ and the characteristic Equation (least common denominator polynomial) of $\mathbf{P_e}(\mathrm{j}\omega)$. Then, for any nonsingular $l \times l$ polynomial matrix $\mathbf{P}'_{\mathbf{e}}(\mathrm{j}\omega)$, a diagonal matrix $\mathbf{D}(\mathrm{j}\omega)$ can always be determined, such that for r_{max} = maximum power of ω in the numerator terms of $\mathbf{P}'_{\mathbf{e}}(\mathrm{j}\omega)$,

$$\mathbf{P}'_{\mathbf{e}}(\mathrm{j}\omega) = \mathbf{D}(\mathrm{j}\omega)[I_{l\times l}(j\omega)^{r_{max}} + A_{r_{max}-1}(j\omega)^{r_{max}-1} + \ldots A_1(j\omega) + A_0] \qquad (2.49)$$

where the maximum power of the polynomials of any i^{th} column of $\mathbf{P}'_{\mathbf{e}}(\mathbf{j}\omega)$ is along the i^{th} diagonal of $\mathbf{D}(\mathbf{j}\omega)$. It follows that

$$det(\mathbf{P}'_{\mathbf{e}}(\mathbf{j}\omega)) = det(\mathbf{D}(\mathbf{j}\omega)[I_{l\times l}(j\omega)^{r_{max}} + A_{r_{max}-1}(j\omega)^{r_{max}-1} + \ldots A_1(j\omega) + A_0]) \quad (2.50)$$

Now, an equivalent expression for the braketed term of the previous equation is given by

$$det((j\omega)I_{l\times l} - L) = \begin{pmatrix} 0_{l\times l} & \ldots & 0_{l\times l} & -A_0 \\ I_{l\times l} & \ldots & 0_{l\times l} & -A_1 \\ \vdots & \ddots & \vdots & \vdots \\ 0_{l\times l} & \ldots & I_{l\times l} & -A_{r_{max}-1} \end{pmatrix} \quad (2.51)$$

Hence, it is concluded that

$$det(\mathbf{P}'_{\mathbf{e}}(\mathbf{j}\omega)) = det(\mathbf{D}(\mathbf{j}\omega))det((j\omega)I_{l\times l} - L) \quad (2.52)$$

and for r_{min} equal to the smallest power of ω in $\mathbf{D}(\mathbf{j}\omega)$, that eigenvalues of $\mathbf{P}'_{\mathbf{e}}(\mathbf{j}\omega)$ are given by the eigenvalues of L after excluding $r_{max} - r_{min}$ zero eigenvalues added by the formation of the L matrix. The determination of whether the v_{ij} are MP can be made, therefore, by determining if the remaining eigenvalues of L lie in the LHP.

For example, for the following $\mathbf{P}'_{\mathbf{e}}(\mathbf{j}\omega)$ polynomial matrix

$$\mathbf{P'_e(j\omega)} = \begin{pmatrix} -\omega^2 + 4j\omega + 4 & j\omega + 2 \\ 1 & j\omega + 2 \end{pmatrix}$$

$\mathbf{P'_e(j\omega)}$ is rewritten as $\mathbf{P'_e(j\omega)} = \mathbf{D(j\omega)}\,[I_{l\times l} + A_1(j\omega)^{-1} + A_0(j\omega)^{-2}]$ to yield

$$\mathbf{P'_e(j\omega)} = \begin{pmatrix} (j\omega)^2 & 0 \\ 0 & (j\omega) \end{pmatrix} \left(\begin{pmatrix} 1 & 0 \\ 0 & 1 \end{pmatrix} + \begin{pmatrix} 4 & 1 \\ 1 & 2 \end{pmatrix} (j\omega)^{-1} + \begin{pmatrix} 4 & 2 \\ 0 & 0 \end{pmatrix} (j\omega)^{-2} \right)$$

So that for

$$L = \begin{pmatrix} 0_{2\times 2} & -A_0 \\ I_{2\times 2} & -A_1 \end{pmatrix} = \begin{pmatrix} 0 & 0 & -4 & -2 \\ 0 & 0 & 0 & 0 \\ 1 & 0 & -4 & -1 \\ 0 & 1 & -1 & -2 \end{pmatrix}$$

the $det((j\omega)I - L)$ yields eigenvalues of 0, -1, -2, and - 3. Excluding $r_{max} - r_{min} = 2 - 1$ zero eigenvalues (i.e., excluding the only zero eigenvalue), we determine that eigenvalues of $det(\mathbf{P'_e(j\omega)})$ are -1, -2, and -3 and hence the v_{ij} are MP.

Again, the method appears useful in screening out inappropriate selections of $\mathbf{Q(j\omega)}$, but it appears unlikely that the method can be incorporated into the selection process of $\mathbf{Q(j\omega)}$.

To conclude, methods are available for determining if the (m_{ij}) of $\mathbf{P_e^{-1}(j\omega)}$ are MP by evaluating the $det(\mathbf{P_e(j\omega)})$. However, since the available methods appear to have applicability only after the selection of the $\mathbf{Q(j\omega)}$ compensator is made, the methods can be expected to see little use. If the evaluation is done after the selection of the $\mathbf{Q(j\omega)}$ matrix, numerical evaluations of $det(\mathbf{P_e(j\omega)})$ are simpler and quicker.

2.9 *Selection of* $\mathbf{Q}(j\omega)$ *for MIMO QFT Designs*

In this section, QFT design requirements are examined to determine optimal $\mathbf{Q}(j\omega)$. As the intent of this study is to concentrate on the selection of a $\mathbf{Q}(j\omega)$ that minimizes the difference between the two sides of Equation (1.1), it is imperative that $\mathbf{P}(j\omega)$ be first fixed ($\mathbf{P}(j\omega) \in \mathcal{P}(j\omega)$). Hence, for purposes of this study the objective is established by specifying that $\mathbf{Q}(j\omega)$ is to minimize Equation (1.1) with respect to the healthy plant.

The first criterion for $\mathbf{Q}(j\omega)$ is that the product of $\mathbf{P}(j\omega)$ and $\mathbf{Q}(j\omega)$ be a square matrix. This constraint is stated first since it allows us to proceed under the asumption that $\mathbf{P}(j\omega)\mathbf{Q}(j\omega)$ is a square matrix. Obviously, for any $l \times m$ matrix $\mathbf{P}(j\omega)$, we can always find an $m \times l$ $\mathbf{Q}(j\omega)$ that yields a square $l \times l$ $\mathbf{P_e}(j\omega)$.

Before proceeding to the second criterion, some matrix equivalents are established. While we proceed by use of an example, similar statements can be made for any nonsquare $\mathbf{P}(j\omega)$ and $\mathbf{Q}(j\omega)$ matrices whose product is square by applying the Binet-Cauchy formula (7:5-19).

Consider a 2×3 matrix of transfer function elements $\mathbf{P}(j\omega)$, such that

$$\mathbf{P}(j\omega) = \begin{pmatrix} p_{11} & p_{12} & p_{13} \\ p_{21} & p_{22} & p_{23} \end{pmatrix}$$

and a generalized compensator $\mathbf{Q}(j\omega)$, such that

$$\mathbf{Q}(j\omega) = \begin{pmatrix} q_{11} & q_{12} \\ q_{21} & q_{22} \\ q_{31} & q_{32} \end{pmatrix}$$

The product $\mathbf{P}(j\omega)\mathbf{Q}(j\omega)$ is given by

$$\mathbf{P}(j\omega)\mathbf{Q}(j\omega) = \begin{pmatrix} p_{11}q_{11} + p_{12}q_{21} + p_{13}q_{31} & p_{11}q_{12} + p_{12}q_{22} + p_{13}q_{32} \\ p_{21}q_{11} + p_{22}q_{21} + p_{23}q_{31} & p_{21}q_{12} + p_{22}q_{22} + p_{23}q_{32} \end{pmatrix} \tag{2.53}$$

The right hand side of Equation (2.53) is rewritten to yield

$$\begin{aligned} \sum_{i=1}^{9} P_i Q_i &= P_1Q_1 + P_2Q_2 + P_3Q_3 + P_4Q_4 + P_5Q_5 \\ &\quad + P_6Q_6 + P_7Q_7 + P_8Q_8 + P_9Q_9 \end{aligned} \tag{2.54}$$

Note that Equation (2.54) cannot be set equal to the right hand side of Equation (2.53) without first defining an equivalence relationship. This is done later. For now, continue by noting that the P_i and Q_i of Equation (2.54) are given by

$$P_1Q_1 = P(s)\begin{pmatrix} q_{1_{11}} & q_{1_{12}} \\ q_{1_{21}} & q_{1_{22}} \\ 0 & 0 \end{pmatrix} = \begin{pmatrix} p_{11} & p_{12} \\ p_{21} & p_{22} \end{pmatrix}\begin{pmatrix} q_{1_{11}} & q_{1_{12}} \\ q_{1_{21}} & q_{1_{22}} \end{pmatrix} \tag{2.55}$$

$$P_2Q_2 = P(s)\begin{pmatrix} q_{2_{11}} & q_{2_{12}} \\ 0 & 0 \\ q_{2_{31}} & q_{2_{32}} \end{pmatrix} = \begin{pmatrix} p_{11} & p_{13} \\ p_{21} & p_{23} \end{pmatrix}\begin{pmatrix} q_{2_{11}} & q_{2_{12}} \\ q_{2_{31}} & q_{2_{32}} \end{pmatrix} \tag{2.56}$$

$$P_3Q_3 = P(s)\begin{pmatrix} 0 & 0 \\ q_{3_{21}} & q_{3_{22}} \\ q_{3_{31}} & q_{3_{32}} \end{pmatrix} = \begin{pmatrix} p_{12} & p_{13} \\ p_{22} & p_{23} \end{pmatrix}\begin{pmatrix} q_{3_{21}} & q_{3_{22}} \\ q_{3_{31}} & q_{3_{32}} \end{pmatrix} \tag{2.57}$$

$$P_4Q_4 = P(s)\begin{pmatrix} q_{4_{11}} & 0 \\ 0 & q_{4_{22}} \\ q_{4_{31}} & q_{4_{32}} \end{pmatrix} \quad P_5Q_5 = P(s)\begin{pmatrix} 0 & q_{5_{12}} \\ q_{5_{21}} & 0 \\ q_{5_{31}} & q_{5_{32}} \end{pmatrix}$$

$$P_6Q_6 = P(s)\begin{pmatrix} q_{6_{11}} & q_{6_{12}} \\ 0 & q_{6_{22}} \\ q_{6_{31}} & 0 \end{pmatrix} \quad P_7Q_7 = P(s)\begin{pmatrix} q_{7_{11}} & q_{7_{12}} \\ q_{7_{21}} & 0 \\ 0 & q_{7_{32}} \end{pmatrix}$$

$$P_8Q_8 = P(s)\begin{pmatrix} q_{8_{11}} & 0 \\ q_{8_{21}} & q_{8_{22}} \\ 0 & q_{8_{32}} \end{pmatrix} \quad P_9Q_9 = P(s)\begin{pmatrix} 0 & q_{9_{12}} \\ q_{9_{21}} & q_{9_{22}} \\ q_{9_{31}} & 0 \end{pmatrix}$$

Note that only the first three products can actually be formed using a square P_i. The 2×2 P_i for $i \in (4,5,6,7,8,9)$ do not truly exist. Let the 3×2 Q_i matrices be denoted as Q_i'. Next observe that each of the Q_i' for $i \in (4,5,6,7,8,9)$ is just a linear combination of the Q_i' for $i \in (1,2,3)$. As such, only the first three elements of equation (2.55) are needed to span the space of achievable $\mathbf{Q}(\mathrm{j}\omega)$. In general for an $l \times m$ $\mathbf{P}(\mathrm{j}\omega)$ and an $m \times l$ $\mathbf{Q}(\mathrm{j}\omega)$, the Binet-Cauchy theorem yields m^2 P_iQ_i combinations of which only m are needed to span the space of all possible $\mathbf{P}(\mathrm{j}\omega)\mathbf{Q}(\mathrm{j}\omega)$ products.

That only the first three P_iQ_i for $i \in (1,2,3)$, are needed to span the space of possible $\mathbf{P}(\mathrm{j}\omega)\mathbf{Q}(\mathrm{j}\omega)$ is verified by forming the sum of the P_iQ_i of equations (2.55)

through (2.57). The sum results in Equation (2.54) with the q_{ij} elements of Equation (2.54) given by

$$\begin{aligned} q_{11} &= [q_{1_{11}} + q_{2_{11}}] \\ q_{12} &= [q_{1_{12}} + q_{2_{12}}] \\ q_{21} &= [q_{1_{21}} + q_{3_{21}}] \\ q_{22} &= [q_{1_{22}} + q_{3_{22}}] \\ q_{31} &= [q_{2_{31}} + q_{3_{31}}] \\ q_{32} &= [q_{2_{32}} + q_{3_{32}}] \end{aligned} \tag{2.58}$$

As such, the P_i for $i \in (4,5,6,7,8,9)$ are eliminated from further consideration.

The purpose in breaking up the product is to define a set of P_iQ_i matrices such that any $\mathbf{P_e}(\mathbf{j}\omega) = \mathbf{P}(\mathbf{j}\omega)\mathbf{Q}(\mathbf{j}\omega)$ can be formed as a linear combination of several P_iQ_i matrices. The objective is to define selection criteria for $\mathbf{Q}(\mathbf{j}\omega)$ on the on the basis of the square P_iQ_i matrices. A desirable $\mathbf{Q}(\mathbf{j}\omega)$ is then formed using the desirable Q_i. Note that in seeking to achieve this objective that Equation (2.55) potentially yields $m^2 * \mathbf{P_e}(\mathbf{j}\omega)$, since Equation (2.55) contains m^2 versions of $\mathbf{P_e}(\mathbf{j}\omega)$. If only the P_i for $i \in (1,2,3)$ are retained, then the relationship between equations (2.54) and (2.55) is given by

$$\mathbf{P}(\mathbf{j}\omega)\mathbf{Q}(\mathbf{j}\omega) = \frac{1}{n}\sum_{i=1}^{n} P_iQ_i, \quad n = 3 \tag{2.59}$$

Note however, that the value of n in Equation (2.59) is reduced if additional P_i are eliminated. For example, if P_2 were not invertible or failed to satisfy the

remaining QFT criteria, then P_2 would be eliminated from further consideration and the value of n in Equation (2.59) reduced to $n = 2$.

The second criterion is that the product $\mathbf{P}(\mathrm{j}\omega)\mathbf{Q}(\mathrm{j}\omega) = \mathbf{P_e}(\mathrm{j}\omega)$ be non-singular over the entire range of plant uncertainties. A sufficient condition for implementing this requirement is to require that each of the P_iQ_i combinations be nonsingular.

The impact of a P_i matrix for $i \in (1,2,3)$ whose determinant $det(P_i)$ does go to zero for certain plant parameter variations is next determined. Note that this criterion is applied to functions in the P_i matrices and not to evaluations of the functions at certain frequencies.

Assume a P_i, $i \in (1,2,3)$ is singular. If P_i is singular, then for some plant in the set of possible plants, $det(P_i) = 0$. As each P_i is square, the product rule for determinants applies. Hence, for P_iQ_i combinations where $i \in (1,2,3)$,

$$det(P_iQ_i) = det(P_i)det(Q_i) \tag{2.60}$$

Based on the above result, we conclude that if $det(P_i)$, $i \in (1,2,3)$ does go to zero, then no Q_i eliminates the zero. Conversely, it also follows that if these three P_i are nonsingular, then any nonsingular Q_i ensures that the product P_iQ_i satisfies the second criterion. To proceed, it must be assumed that at least one P_i of Equation (2.59) is invertible.

The third criterion noted in Chapter I is that the product $\mathbf{P}(\mathrm{j}\omega)\mathbf{Q}(\mathrm{j}\omega)$ satisfy a diagonal dominance condition as $\omega \to \infty$ over the entire range of plant parameter variations. This condition ensures that the diagonal transfer functions dominate the plant's response at high frequencies. A more restrictive version of this requirement is Rosenbrock's dominance condition that requires that the diagonal transfer functions dominate the plant's response at all frequencies.

Note that diagonal dominance in QFT differs from that usually referred to in linear algebra courses. In this case, diagonal dominance is that characteristic of a matrix that is observed when the eigenvalues of the matrix satisfy Gershgorin's "circle theorem" (17:386-387).

The application of the criterion to $\mathbf{P_e}(j\omega)$ or to the P_i $i \in (1,2,3)$ is readily done by evaluating transfer function elements of the matrices over a desired frequency range and then applying magnitude conditions detailed in (7) and (3). For 2×2 matrices, the diagonal dominance condition requires that

$$|p_{e_{11}} p_{e_{22}}| \geq |p_{e_{12}} p_{e_{21}}| \tag{2.61}$$

For matrices of any higher dimension, (7) provides the necessary information. It follows that if any P_iQ_i that is diagonally dominant is added to any other P_jQ_j that is also diagonally dominant, then the resulting sum is also diagonally dominant.

Once a Q_i matrix is selected, then the matrix product P_iQ_i is evaluated over some frequency range to determine the extent to which each P_iQ_i combination is diagonally dominant. As such, we are able to select for QFT design purposes, the diagonally dominant P_iQ_i.

Ideally, the selection process for $\mathbf{Q}(j\omega)$ yields a $\mathbf{P_e}(j\omega)$ that satisfies Rosenbrock's diagonal dominance condition. In such cases, design efforts are reduced and the resultant design is simplified. However, selecting $\mathbf{Q}(j\omega)$ to primarily accomplish this objective entails abandoning efforts to select $\mathbf{Q}(j\omega)$ on the basis of a prespecified $\mathbf{P_e}(j\omega)$ matrix.

The fourth criterion requires that roots of $det(\mathbf{P_e}(j\omega))$ lie in the LHP (i.e., that the $(m_{ij})^{-1} = v_{ij}$ be MP, where the m_{ij} are elements of $\mathbf{P_e^{-1}}(j\omega)$). This criterion cannot be applied when the plant transfer matrix is nonsquare. However, in the form

of a set of squared-down versions P_iQ_i, the criterion is readily applied. As such, the P_iQ_i combinations can be evaluated to weed out undesirable choices of Q_i.

A summary point about the four QFT criterion is now made. Of the four criteria, three are GO-NO GO type of evaluations. Only one of the four, the third criterion concerning diagonal dominance, may be said to be qualitative in nature. As such, it is believed that the selection process should concentrate on the third criterion, reverting back to the three remaining criteria only to the extent necessary to ensure compliance.

Once desirable Q_i are determined, a single $\mathbf{Q}(\mathrm{j}\omega)$ is then formed as the weighted sum of the expanded Q_i'. Weighting matrices W_i whose sum equals $I_{l\times l}$ are used for this purpose. The W_i are restricted to the use of scalar values in order to preclude further changes in the MP characteristics of the equivalent plant. The QFT design process is then entered using a single $\mathbf{Q}(\mathrm{j}\omega)$.

The fact that choosing the W_i to satisfy $\sum W_i = I_{l\times l}$ yields $\mathbf{P_e}(\mathrm{j}\omega)$ is readily demonstrated for the case of invertible P_i by the following set of equalities. The Q_i satisfying Equation (1.1) are given by $Q_i = P_i^{-1}P_e$ since the P_i must be invertible.

$$\begin{aligned} P(Q_1'W_1 + Q_2'W_2 + Q_3'W_3) &= PQ_1'W_1 + PQ_2'W_2 + PQ_3'W_3 \\ &= P_1P_1^{-1}P_eW_1 + P_2P_2^{-1}P_eW_2 + P_3P_3^{-1}P_eW_3 \\ &= P_e(W_1 + W_2 + W_3) \\ &= P_e \end{aligned}$$

Alternately QFT designs can be determined for each of the P_iQ_i for retained P_i and the individual designs implemented in parallel. With the QFT process completed using three versions of P_iQ_i, design implementation occurs as shown in Figure 2.3.

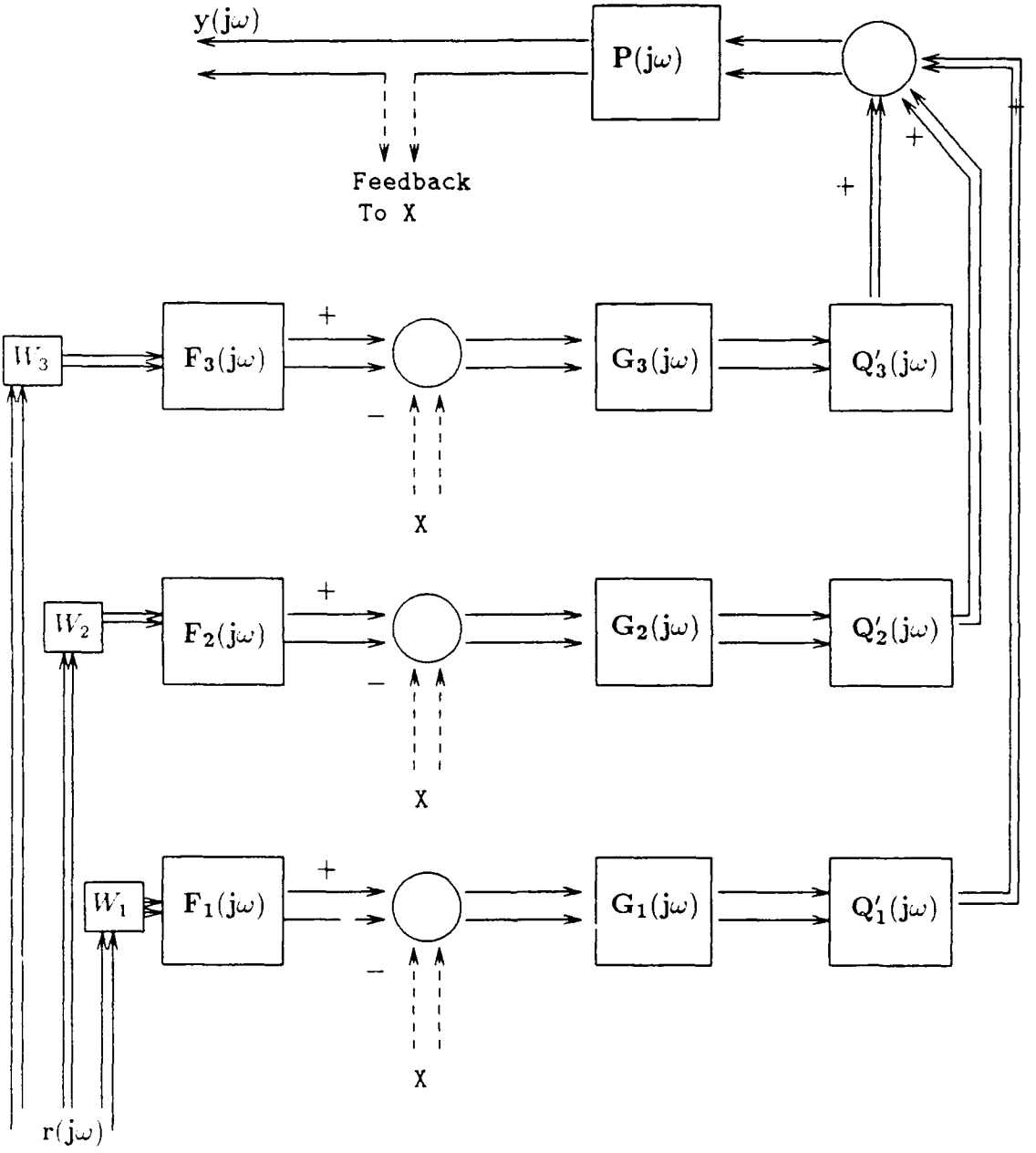

Figure 2.8. The QFT Compensated Plant with W Weighting Matrices

The W_i weightings are then selected to achieve an overall best compensating system. It is anticipated that if tradeoffs are necessary in the selection of the W_i, that the tradeoffs are more visible in a post-QFT environment.

The process of H_2 or H_∞-norm minimization is accomplished in the absence of other design criteria for establishing tradeoffs between the W_i. As each P_i retained to this point is assumed invertible, it follows that the Q_i are already H_2 and H_∞-norm minimal with respect to the healthy plant. As such, the use of H_2 or H_∞-norm minimization is used to address the entire set of possible plants. As there is no mathematical formulation available for this purpose, the process of minimizing the H_2 or H_∞-norm over the set of all $\mathbf{P_e}(\mathrm{j}\omega) \in \mathcal{P}_\mathbf{e}(\mathrm{j}\omega)$ is done by trial and error selections of the W_i. However, the process is applicable only if transfer function elements of the retained P_i are stable for all plant parameter variations.

Before concluding this section, the idea of abandoning a prespecified equivalent plant and instead seeking to select $\mathbf{Q}(\mathrm{j}\omega)$ to make the product $\mathbf{P}(\mathrm{j}\omega)\mathbf{Q}(\mathrm{j}\omega)$ satisfy Rosenbrock's diagonal dominance condition is examined. The examination is conducted by examining the impact of two different $\mathbf{Q}(\mathrm{j}\omega)$ on the diagonal dominance characteristics of $\mathbf{P}(\mathrm{j}\omega)\mathbf{Q}(\mathrm{j}\omega)$ for $P_i \in (1,2,3)$.

First, a diagonal Q_i is assumed. For explanation simplicity, it is assumed, without loss of generality, that the P_i being used is P_2. The product of P_2 and an assumed diagonal Q_2 is given by

$$P_2 Q_2 = \begin{pmatrix} p_{11} & p_{12} \\ p_{21} & p_{22} \end{pmatrix} \begin{pmatrix} q_{2_{11}} & 0 \\ 0 & q_{2_{22}} \end{pmatrix} \tag{2.62}$$

Carrying out the product and applying the diagonal dominance condition Equation (2.57), the following is obtained.

$$|(p_{11}q_{2_{11}})(p_{22}q_{2_{22}})| \geq |(p_{12}q_{2_{22}})(p_{21}q_{2_{11}})|$$
$$|q_{2_{11}}q_{2_{22}}|\,|p_{11}p_{22}| \geq |q_{2_{11}}q_{2_{22}}|\,|p_{12}p_{21}|$$

and it is concluded that a diagonal Q_i provides frequency sensitive scaling of each side of the inequality, but does nothing to alter the diagonal dominance characteristics of the P_i matrix.

Now, a Q_i whose numerator terms are the conjugates of numerators of elements of P_i and whose common denominator terms are the same common denominator terms of P_i is next investigated. To express both the P_i and the Q_i elements in a common frame, let den_p represent the common denominator term of P_i and den_q the common denominator terms of Q_i. Further let n_{ij} represent the numerator terms of P_i. Again, for explanation simplicity, it is assumed that the P_i being used is P_2.

$$P_2Q_2 = \begin{pmatrix} n_{11}/den_p & n_{12}/den_p \\ n_{21}/den_p & n_{22}/den_p \end{pmatrix} \begin{pmatrix} \overline{n_{11}}/den_q & \overline{n_{12}}/den_q \\ \overline{n_{21}}/den_q & \overline{n_{22}}/den_q \end{pmatrix} \tag{2.63}$$

Carrying out the product and applying the diagonal dominance condition, the following is obtained.

$$|n_{11}\overline{n_{11}}n_{22}\overline{n_{22}} + n_{12}\overline{n_{21}}n_{21}\overline{n_{12}}| \geq |n_{12}\overline{n_{11}}p_{21}\overline{n_{22}} + n_{11}\overline{n_{12}}n_{22}\overline{n_{21}}| \tag{2.64}$$

where the common denominator terms have been removed since they only alter the

scaling of the inequality. But as the right hand side of the inequality is the sum of a function and its complex congugate, the right hand side satisfies

$$|2 * Re[n_{12}\overline{n_{11}}n_{21}\overline{n_{22}}]| = |n_{12}\overline{n_{11}}n_{21}\overline{n_{22}} + n_{11}\overline{n_{12}}n_{22}\overline{n_{21}}| \tag{2.65}$$

both sides of the inequality are equivalently expressed by

$$| \, |n_{11}n_{22}|^2 + |n_{12}n_{21}|^2 \, | \geq | \, 2 * \sqrt{|n_{12}|^2 \, |n_{11}|^2 \, |n_{21}|^2 \, |n_{22}|^2} \, | \tag{2.66}$$

Removing the excess outer absolute value bars and squaring both sides of the previous inequality, the following results

$$|n_{11}n_{22}|^4 + 2 * |n_{11}n_{22}n_{12}n_{21}|^2 + |n_{12}n_{21}|^4 \geq 2 * |n_{12}n_{11}n_{21}n_{22}|^2 \tag{2.67}$$

which implies that

$$|n_{11}n_{22}|^4 + |n_{12}n_{21}|^4 \geq 0 \tag{2.68}$$

and it is concluded that this Q_i guarantees that Rosenbrock's diagonal dominance condition is at least satisfied for the healthy plant. Hence, we are able to define conditions for ineffective and effective Q_i for improving the diagonal dominance of a P_i. However, the application of the latter Q_i entails some modification since a

selection based on the healthy plant may drive the equivalent plant matrices $\mathbf{P_e}(j\omega) \in \mathcal{P}_e(j\omega)$ to be NMP.

2.10 Summary

The following summarizes material in this chapter.

1. Elements needed to determine the singular value decomposition of a matrix of transfer functions are obtainable. In general, however, the transfer function elements are not real-rational functions in $j\omega$ and their use in determining solutions to the model-matching problem is limited.
2. The application of QFT to MIMO plants relies on defining a multiple-input, single-output (MISO) equivalence mapping. QFT constraints stem from this mapping.
3. Methods are available for determining if the (m_{ij}) of $\mathbf{P_e^{-1}}(j\omega)$ are MP for all plant parameter variations after a $\mathbf{Q}(j\omega)$ has been selected. The most appropriate method, however, remains the numerical evaluation of $det(\mathbf{P_e}(j\omega))$ for different plants $\mathbf{P_e}(j\omega) \in \mathcal{P}_e(j\omega)$. None of the methods available for determining if the (m_{ij}) of $\mathbf{P_e^{-1}}(j\omega)$ are MP is readily adaptable to the forming of a mathematical relationship between the MP criterion of QFT and a desire to minimize either the H_2 or H_∞-norm of the set of all projected plants about some nominal plant.
4. Of the four constraints, only diagonal dominance may be said to be qualitative in nature. As such, it is believed that the selection process should concentrate on satisfying diagonal dominance over the largest bandwidth possible (with the objective of achieving Rosenbrock's diagonal dominance condition), and reverting back to the three remaining criteria only to the extent necessary to ensure compliance. To do so, however, requires abandoning a prespecified $\mathbf{P_e}(j\omega)$.

5. Breaking up the product of $\mathbf{P}(j\omega)\mathbf{Q}(j\omega)$ to define a set of P_iQ_i matrices satisfying $\mathbf{P_e}(j\omega) = \mathbf{P}(j\omega)\mathbf{Q}(j\omega)$ provides a number of insights. QFT designs can be accomplished on a single $\mathbf{Q}(j\omega)$ after summing the nonsquare Q_i' or on individual P_iQ_i and then implementing the results in parallel.

6. As only invertible P_i are retained for QFT design, the Q_i are determined using P_i^{-1}. As such, each Q_i is H_2 and H_∞-norm minimal for the healthy plant. If the design objective is to minimize the H_2 or H_∞-norm over the entire set of possible plants, then it is suggested that the process of minimizing the norm be done using a trial and error approach. This process, however, effectively redefines the plant used to obtain each Q_i from the healthy plant to that nominal plant which minimizes deviations from nominal for the set of possible plants with respect to the selected norm criteria. Since no mathematical formulation is available for integrating the norm-minimization requirement with a summation of P_iQ_i equivalent plants, either a trial and error aproach in selecting $\mathbf{Q}(j\omega)$ is used or each individual Q_i of P_iQ_i is selected to norm-minimize the P_iQ_i and then the resultant designs implemented in parallel. Finally, to apply norm-minimization criteria, it is noted that transfer function element of $\mathbf{P}(j\omega)$ must be stable for all plant parameter variations.

7. To define the best overall compensating system, weighting matrices W_i are introduced. Elements of the W_i are chosen to satisfy $\sum W_i = I$ and either overall design requirements for closed-loop plant performance or to minimize the norm-criteria for a sum of P_iQ_i.

8. The use of a diagonal Q_i with an invertible P_i is ineffective. Diagonal Q_i do nothing to alter the diagonal dominance characteristics of a P_i matrix.

9. The use of a Q_i whose numerator terms are the conjugates of numerators of elements of P_i guarantees that Rosenbrock's diagonal dominance condition is satisfied for the healthy plant. The method, however, requires modification to guard against driving equivalent plant matrices $\mathbf{P_e}(j\omega) \in \mathcal{P}_\mathbf{e}(j\omega)$ to be NMP.

III. Flight Controller Design

3.1 Examination of Plant Characteristics

In this chapter, transfer functions are expressed using Laplace transforms. Conditions at the beginning of Chapter II are satisfied; the frequency domain representation of the transfer functions is given by substituting $j\omega$ for s.

The aircraft plant selected for compensation is that of the AFTI/F16 in level flight at 0.9 Mach and at an altitude of 20,000 feet. The objective of the compensation is to maintain effective plant roll rate and yaw rate response despite limited control surface failures. The linearized plant model is described by a state space equation in the following form

$$\dot{x} = Ax + Bu \tag{3.1}$$

$$y = Cx + Du \tag{3.2}$$

where the positive direction of roll, yaw, and sideslip is as shown in Figure 3-1. A description of the state space equation variables follows.

ϕ is the aircraft roll angle in degrees

β is the aircraft sideslip angle in degrees

p is the aircraft roll rate in degrees per second

r is the aircraft yaw rate in degrees per second

δ_a is the aileron deflection in degrees

δ_r is the rudder deflection in degrees

δ_{ht} is the horizontal tail deflection in degrees

The matrices of equations 3.1 and 3.2 follow.

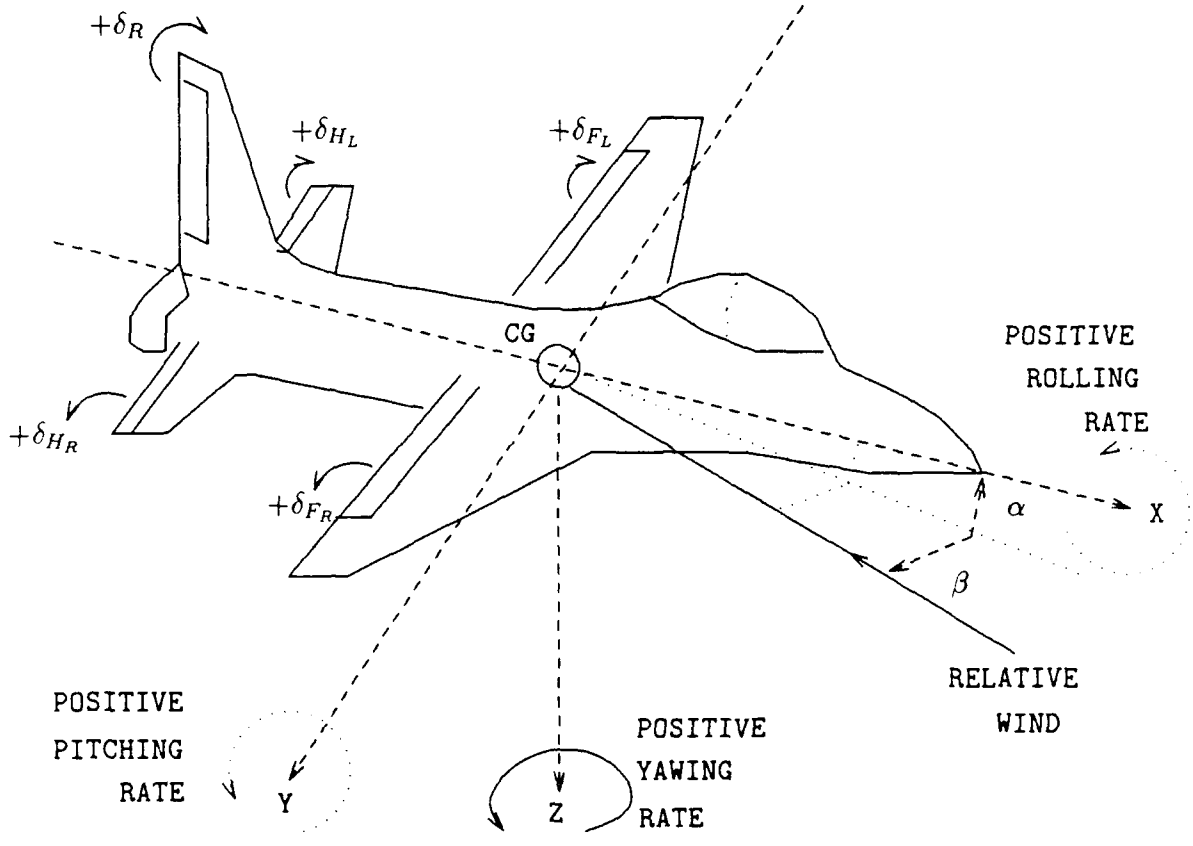

Figure 3.1. Aircraft Plant Directions for Positive Deflections

$$\dot{x} = \begin{pmatrix} \dot{\phi} \\ \dot{\beta} \\ \dot{p} \\ \dot{r} \\ \dot{\delta_a} \\ \dot{\delta_r} \\ \dot{\delta_{ht}} \end{pmatrix}$$

$$u = \begin{pmatrix} \delta_a \\ \delta_r \\ \delta_{ht} \end{pmatrix}$$

$$A = \begin{pmatrix} 0.0000 & 0.0000 & 1.0000 & 0.0000 & 0.0000 & 0.0000 & 0.0000 \\ 0.0345 & -0.3436 & 0.0326 & -0.9976 & -0.0014 & 0.0373 & 0.0266 \\ 0.0000 & -55.2526 & -2.8000 & 0.1457 & -51.0500 & 10.3950 & -50.7290 \\ 0.0000 & 7.2370 & -0.0232 & -0.3625 & -1.2501 & -5.8080 & -5.1371 \\ 0.0000 & 0.0000 & 0.0000 & 0.0000 & -20.0000 & 0.0000 & 0.0000 \\ 0.0000 & 0.0000 & 0.0000 & 0.0000 & 0.0000 & -20.000 & 0.0000 \\ 0.0000 & 0.0000 & 0.0000 & 0.0000 & 0.0000 & 0.0000 & -20.0000 \end{pmatrix}$$

$$B = \begin{pmatrix} 0.0000 & 0.0000 & 0.0000 \\ 0.0000 & 0.0000 & 0.0000 \\ 0.0000 & 0.0000 & 0.0000 \\ 0.0000 & 0.0000 & 0.0000 \\ 20.0000 & 0.0000 & 0.0000 \\ 0.0000 & 20.0000 & 0.00000 \\ 0.0000 & 0.0000 & 20.0000 \end{pmatrix}$$

$$y = \begin{pmatrix} p \\ r \end{pmatrix}$$

$$C = \begin{pmatrix} 0.0000 & 0.0000 & 1.0000 & 0.0000 & 0.0000 & 0.0000 & 0.0000 \\ 0.0000 & 0.0000 & 0.0000 & 1.0000 & 0.0000 & 0.0000 & 0.0000 \end{pmatrix}$$

$$D = \begin{pmatrix} 0.0000 & 0.0000 & 0.0000 \\ 0.0000 & 0.0000 & 0.0000 \end{pmatrix}$$

The matrix of transfer functions is given by $P = C(sI - A)^{-1}B + D$. The transfer function matrix is determined to be of the form

$$P = \begin{pmatrix} p_{11} & p_{12} & p_{13} \\ p_{21} & p_{22} & p_{23} \end{pmatrix} \tag{3.3}$$

Letting den_p be the characteristic equation of P, the elements of P are

$$\begin{aligned} den_p &= (s + 3.9083 \pm j2.9614)(s + .0272)(s + 2.6973)(s + 20) \\ p_{11} &= (-1021)(s)(s + .3541 \pm j2.9273)/den \\ p_{12} &= (207.91)(s)(s - 4.6436)(s + 5.0717)/den \\ p_{13} &= (-1014.58)(s)(s + .3749 \pm j3.5777)/den \\ p_{21} &= (-25)(s + .5461 \perp j3.2533)(s + 1.1119)/den \\ p_{22} &= (-116.178)(s + .3284 \pm j.6928)(s + 2.4822)/den \\ p_{23} &= (-102.742)(s + .6699 \pm j1.5474)(s + 1.5372)/den \end{aligned}$$

For the nominal (healthy) plant, all eigenvalues are in the closed LHP and the system is stable.

When plant variations occur, for example as a result of control surface failures, the plant has the following form. In this alternate form, k_1 represents the effectiveness of the aileron control surfaces δ_a, k_2 the effectiveness of the rudder control surface δ_r, and k_3 the effectiveness of the horizontal tail control surfaces δ_{ht}. The set of all possible plants is represented by $\mathcal{P}$ where for each k_i, $i \in (1,2,3)$, $k_i \in [.8,1]$.

$$\mathcal{P} = \begin{pmatrix} (k_1)p_{11} & (k_2)p_{12} & (k_3)p_{13} \\ (k_1)p_{21} & (k_2)p_{22} & (k_3)p_{23} \end{pmatrix} \tag{3.4}$$

The squared down versions of $\mathcal{P}$ are next examined for diagonal dominance. Only the P_i for $i \in (1,2,3)$ need be examined. This is done to establish the extent to which the three P_i are diagonally dominant. The examination is done as a function of frequency as plant variations occur. The condition for diagonal dominance, Equation (2.62), applies.

Figures 3.1 through 3.3 result. The solid line plots represent the extent of diagonal dominance for the healthy P_i. A positive result indicates that the P_i is diagonally dominant at the indicated frequency while a negative result implies the opposite characteristic. The dotted plot of each figure represents the minimal amount of dominance present as the k_i vary between 1 and .8 in .1 step increments.

For this study, few points are needed to determine diagonal dominance for the given plant because the set of all possible plants described by Equation (3.4) satisfies

$$det \begin{pmatrix} (k_i)p_{1i} & (k_j)p_{1j} \\ (k_i)p_{2i} & (k_j)p_{2j} \end{pmatrix} = (k_i)(k_j)det \begin{pmatrix} p_{1i} & p_{1j} \\ p_{2i} & p_{2j} \end{pmatrix}$$

for any $i \neq j$ and $i, j \in (1,2,3)$. In general, a much more complete evaluation of the determinant for the set of all possible plants is required. Note that it is the requirement that diagonal dominance be satisfied as $\omega \rightarrow \infty$ that drives the choice of P_i and not the relative area above the line denoting where the $det(P_i)$ goes to zero.

Based on Figures 3.1 through 3.3, it is concluded that P_1 and P_2 are diagonally dominant while P_3 is not. However, the transpose of P_3 is diagonally dominant and P_3^T is therefore retained for use in subsequent design steps.

In comparing the three plots, it is noted that the points at which all three plots go to zero occur at the same frequencies. Hence, any linear combination of the three plots retains the same frequency points at which $|p_{i11}p_{i22}| = |p_{i12}p_{i21}|$ for any P_i. This is an important point relative to attempts to select $\mathbf{Q}(j\omega)$ for purposes of ensuring that Rosenbrock's diagonal dominance condition is satisfied over the set of *all possible plants*. The current situation indicates that selecting a Q_i that satisfies Equation (2.63) results is a P_iQ_i that still retains the same frequency points at which $|p_{i11}p_{i22}| = |p_{i12}p_{i21}|$.

An examination of the determinants of each of these three P_i is next conducted. The denominator polynomials den_1, den_2, and den_3 of the determinants of $\mathcal{P}_1$, $\mathcal{P}_2$, and $\mathcal{P}_3$ respectively are

$$
\begin{aligned}
den_1 &= 123815(s)(s+.0272)(s+.2901)(s+2.6973)(s+.3908 \pm j2.9614)(s+20)^4 \\
den_2 &= 79535(s)(s+.0272)(s+.2805)(s+2.6973)(s+.3908 \pm j2.9614)(s+20)^4 \\
den_3 &= 139233(s)(s+.0272)(s+.2932)(s+2.6973)(s+.3908 \pm j2.9614)(s+20)^4
\end{aligned}
$$

As each of the denominator polynomials has only LHP roots, inverting indi-

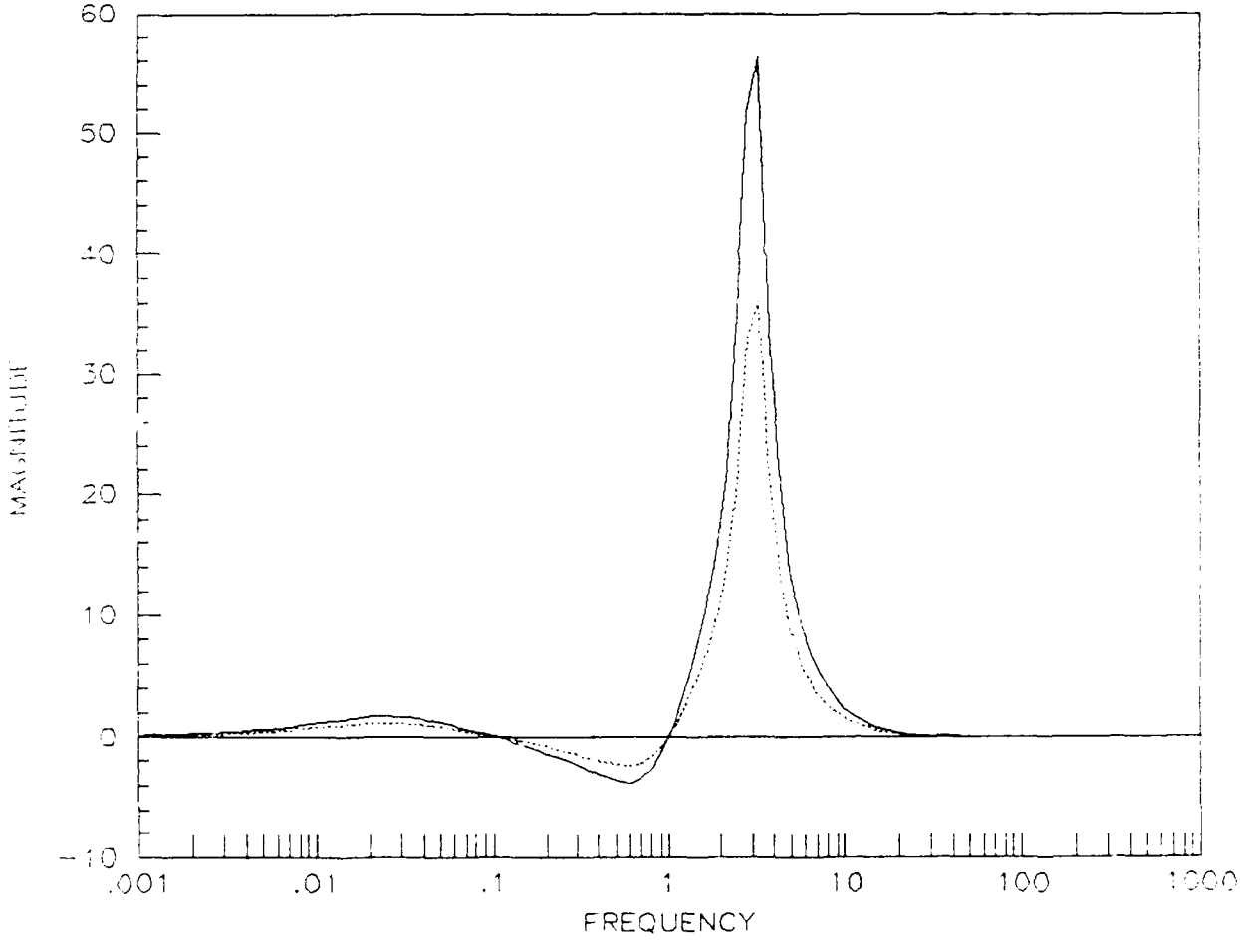

Figure 3.2. Diagonal Dominance of $\mathcal{P}_1(j\omega)$

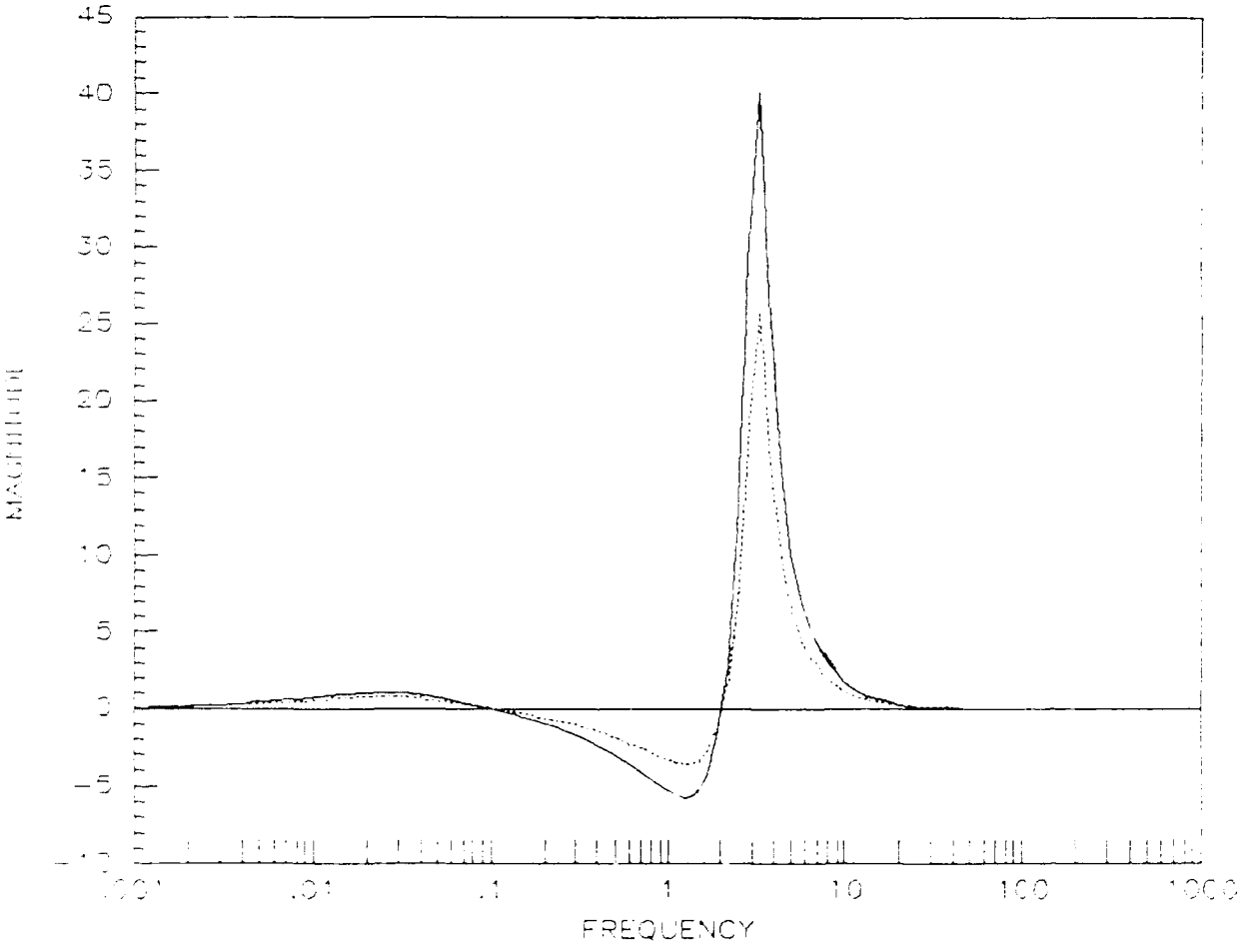

Figure 3.3. Diagonal Dominance of $\mathcal{P}_2(j\omega)$

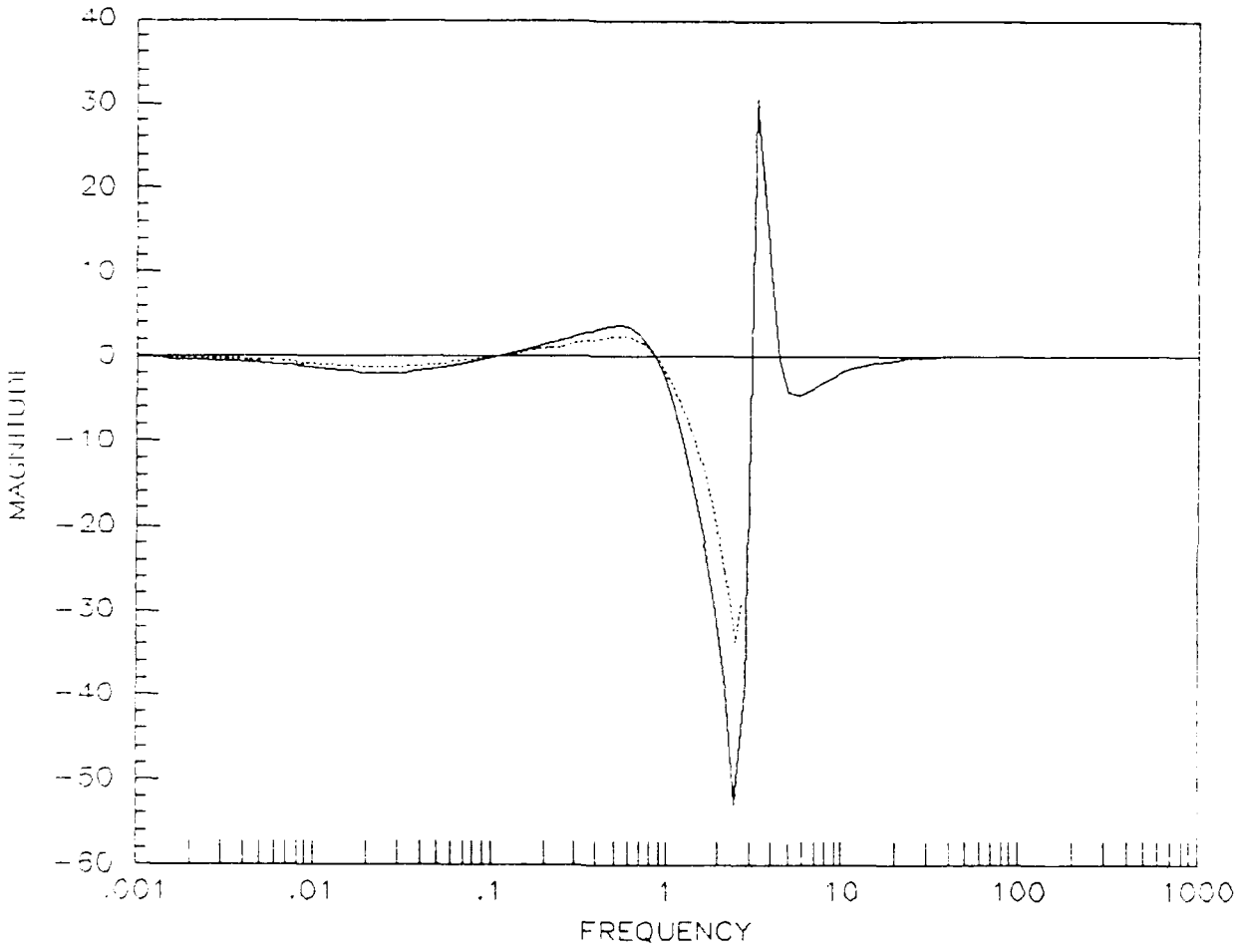

Figure 3.4. Diagonal Dominance of $\mathcal{P}_3(j\omega)$

vidual elements of the P_i^{-1} yields transfer functions that are MP. For the particular plant being used in this study, the denominator polynomials of the determinants of $\mathcal{P}_1$, $\mathcal{P}_2$, and $\mathcal{P}_3$ do not change as plant variations occur. Hence, if the healthy plant P_i are MP, so are the $\mathcal{P}_i$, for $i \in (1,2,3)$.

3.2 *Selection of Equivalent Plant P_e*

From (4:23), the roll mode time constant is to satisfy $T_s \leq 1.0sec$. From (4:22), a requirement that $\omega_{n_d} \geq 1$ rad/sec is also obtained. These requirements are combined with the maximum allowable oscillation requirements of (4:78) to obtain desirable functions for the equivalent plant P_e.

In addition to the performance requirements, the difference in the orders of transfer functions in P_e are selected to coincide with the relative order of transfer functions in P. This is done to ensure that Q_i transfer functions are strictly proper.

The following transfer function is selected for tracking command inputs. The function has a damping ratio $\zeta_d = 0.6$ and natural frequency $\omega_n = 7.5$ rad/sec for the dominant complex pair poles. Hence, $p_{e_{11}}$ is given by

$$p_{e_{11}} = (562.5)/[(s+10)(s^2+9s+56.25)] \tag{3.5}$$

The following transfer function is selected for rejecting undesirable inputs. The rejection transfer function is selected to satisfy diagonal dominance requirements of the P_e while retaining the denominator polynomial of $p_{e_{11}}$.

$$p_{e_{12}} = (s+.001)/[(s+10)^2(s^2+9s+56.25)] \tag{3.6}$$

Based on the above selections for $p_{e_{11}}$ and $p_{e_{12}}$, the desired equivalent plant is formed as

$$P_e = \begin{pmatrix} p_{e_{11}} & p_{e_{12}} \\ p_{e_{12}} & p_{e_{11}} \end{pmatrix} \tag{3.7}$$

Table 3.1. Figures of Merit for P_e

Transfer Function	Peak Value	Final Value	t_p	t_s
$p_{e_{11}}$	1.06142	1.00000	0.665	0.894
$p_{e_{12}}$	0.118E-07	0.267E-11	0.211	2.290

Figures of merit for P_e are as presented in Table 3.1. The settling time t_s and the time to peak t_p are given in seconds. Settling times given are for when the time response is within two percent of its final value.

The time responses for $p_{e_{11}}$ and $p_{e_{12}}$ to a step input are provided as Figures 3.4 and 3.5.

In preparation for obtaining a QFT design, the upper and lower tracking boundary functions are now specified. The transfer functions chosen for the upper tracking function $T_U(s)$ and the lower transfer function establish a region of acceptable responses that satisfy design criteria. In addition, to satisfy QFT design steps, the relative order of $T_U(s)$ must differ from the relative order of $T_L(s)$ by at least 2.

The following function is established as the upper tracking boundary function $T_U(s)$.

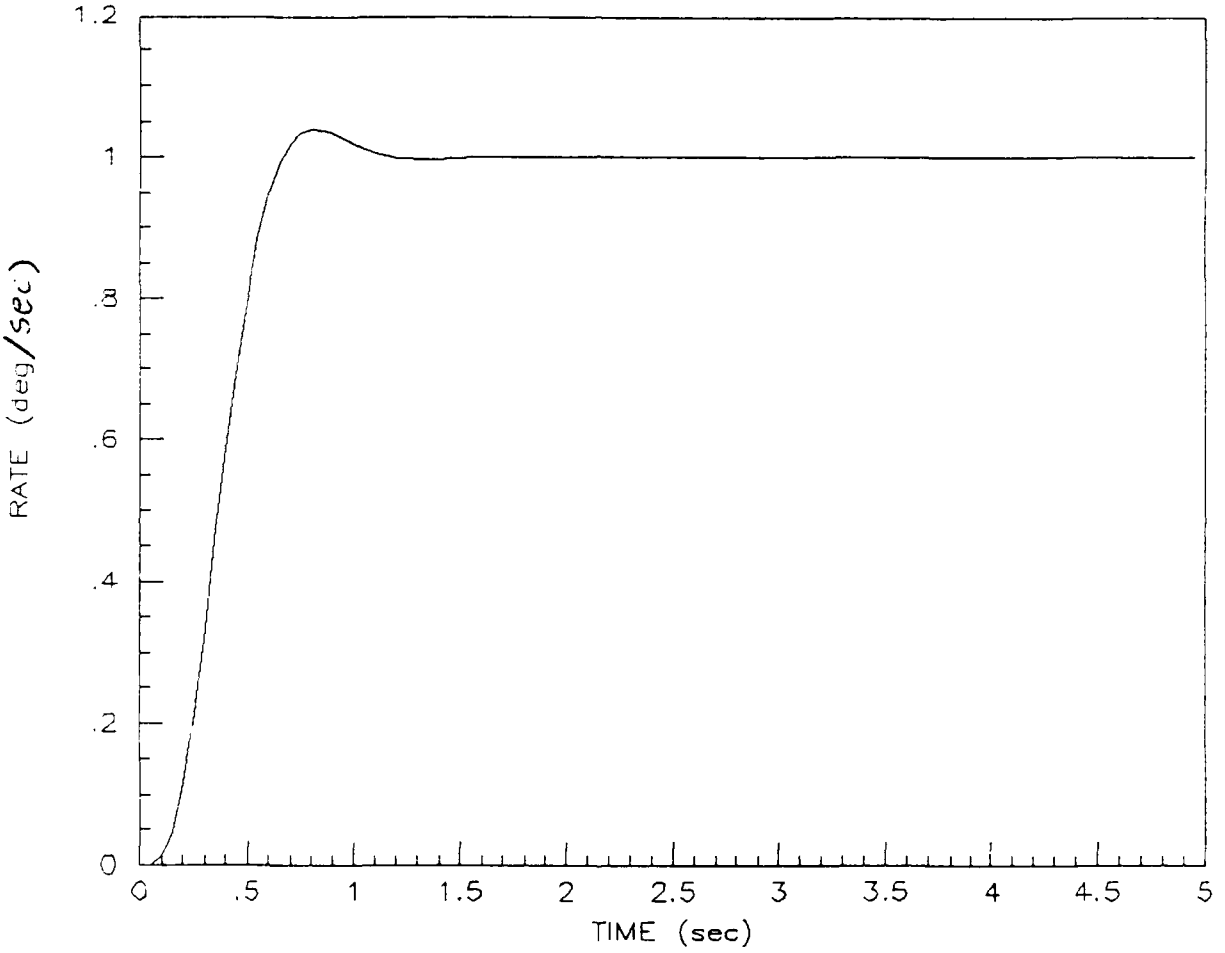

Figure Pe11 Response to Command Step Input

Figure 3.5. Step Input Response of $p_{e_{11}}$

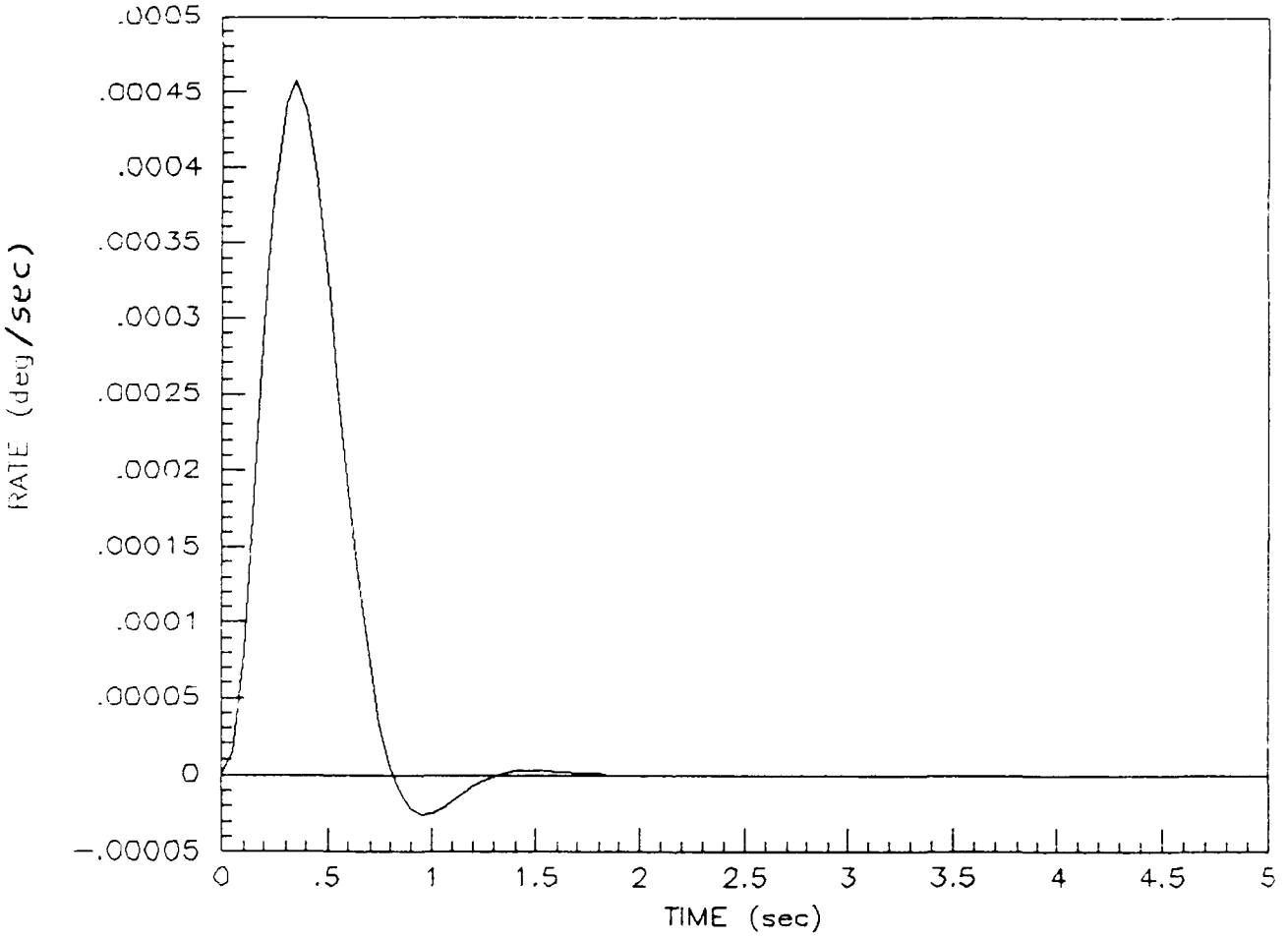

Figure Pe12 Response to Command Step Input

Figure 3.6. Step Input Response of $p_{e_{12}}$

$$T_U(s) = 4(s+16)/[s^2 + 10.4s + 64] = 4(s+16)/[s + 5.2 \pm j6.0795]$$

The following function is established as the lower tracking boundary function $T_L(s)$.

$$T_L(s) = 6400/[s^4 + 36s^3 + 484s^2 + 2880s + 6400] = 6400/[(s+8)^2(s+10)^2]$$

The frequency and step input time responses of the upper and lower tracking functions are provided as Figures 3.6 and 3.7. The central plot in each of these two figures is that of the desirable equivalent plant $p_{e_{11}}$.

3.3 Obtaining and Evaluating the 2×2 Q_i Compensators

The Q_i compensators are next obtained using the healthy 2×2 versions of each P_i for $i \in (1,2,3)$. For the given plant, each of the P_i is invertible so that $Q_i = P_i^{-1} P_e$. Note however,

As acceptable Q_i were not able to be determined, this section continues with a description of steps that were to be taken. The next section is then used to describe efforts that were made to obtain the Q_i.

Assuming the Q_i are obtained, the Q_i' compensators are next determined; each Q_i' is of the form

$$Q_i = \begin{pmatrix} q_{11} & q_{12} \\ q_{21} & q_{22} \\ q_{31} & q_{32} \end{pmatrix} \tag{3.8}$$

Having determined the Q_i' compensators, the product pairs PQ_i' for $i \in (1,2,3)$ are formed to verify achievement of P_e for each cascaded pair. Alternately, verifica-

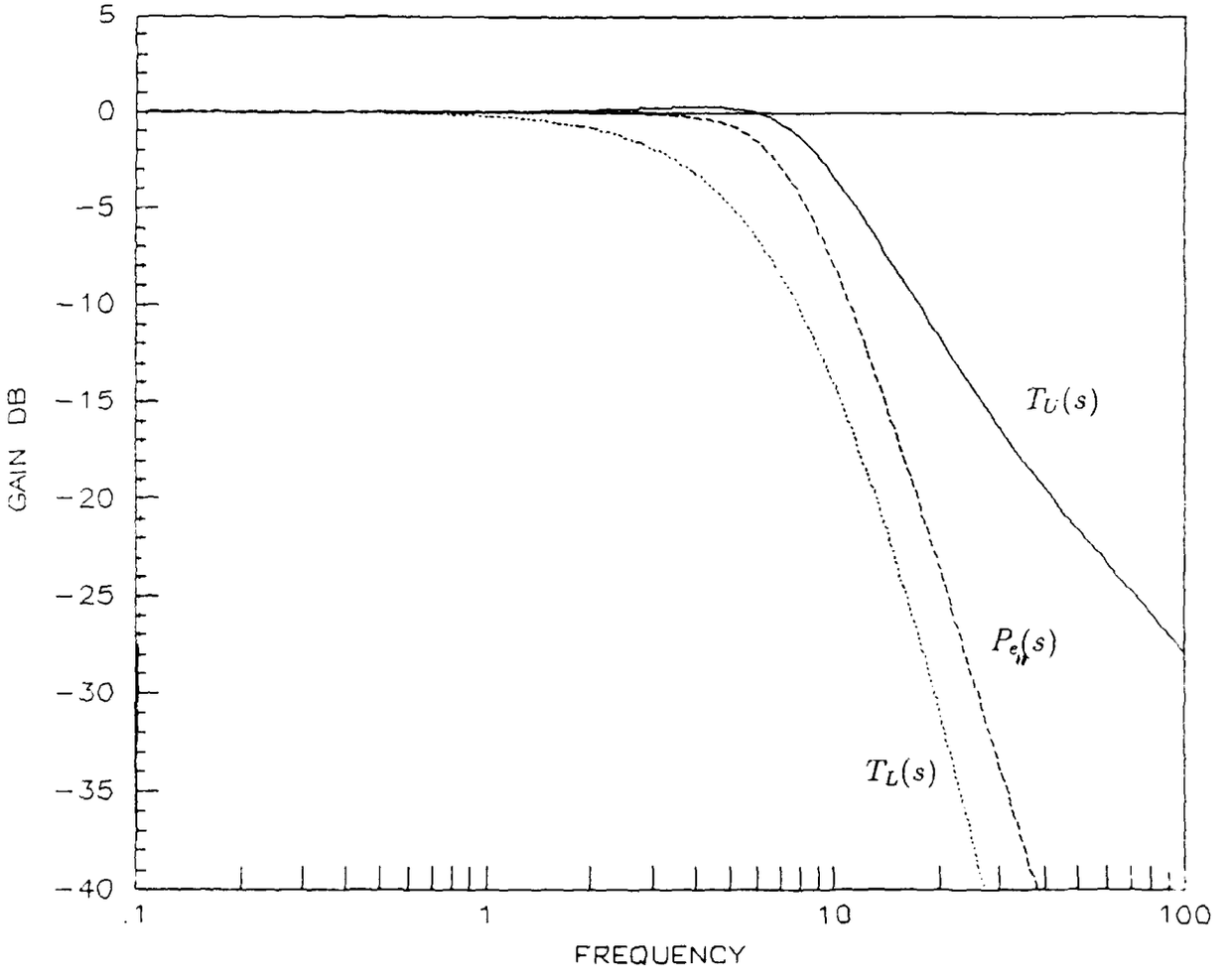

Figure 3.7. Frequency Responses of $T_U(s)$, $T_L(s)$, and $p_{e_{11}}$

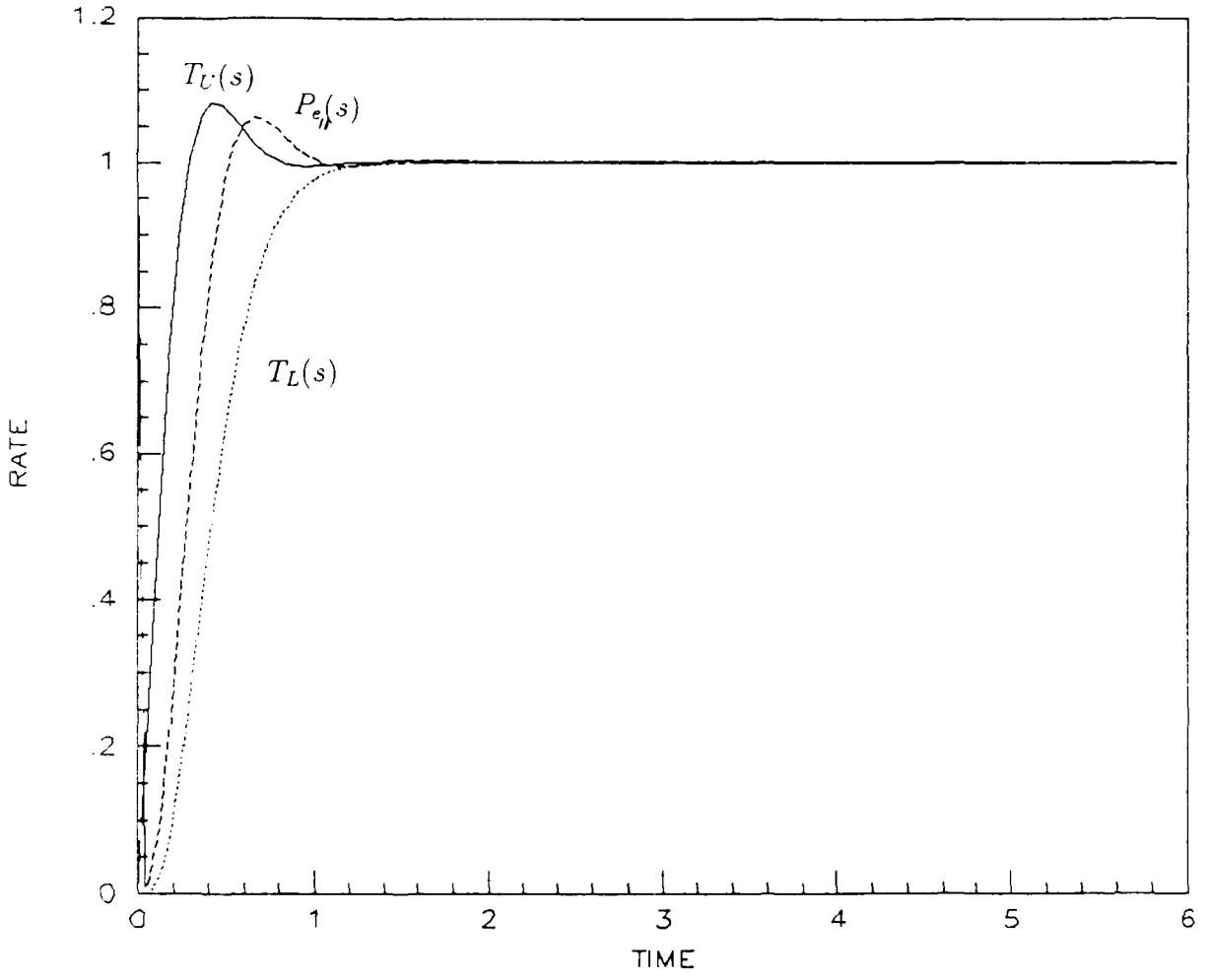

Figure 3.8. Step Input Responses of $T_U(s)$, $T_L(s)$, and $p_{e_{11}}$

tion that acceptable Q_i are achieved is available by obtaining the time responses of the P_iQ_i pairs to step inputs and comparing the step responses to those of P_e.

With the Q_i' in hand, for design implementation using a single $\mathbf{Q}(j\omega)$ matrix, the selection of the W_i weighting matrices is accomplished and $\mathbf{Q}(j\omega)$ is formed as the weighted sum of the Q_i'. The W_i are selected to either satisfy design requirements or to minimize the H_2 or H_∞-norm over the set of all possible plants. With the W_i weightings determined, the QFT design is then accomplished.

3.4 On Obtaining the Q_i Compensators

This section describes efforts made to obtain the Q_i compensators appropriate to converting the healthy plant P_1, P_2, and P_3 into P_e.

In (5) the following operation is provided. For matrices of transfer functions corresponding to the state space realization (A, B, C, D), define $[A, B, C, D] = C * [sI - A]^{-1} * B + D = P$. Then P^{-1} is given by

$$[A, B, C, D]^{-1} = [A - BD^{-1}C, BD^{-1}, -D^{-1}C, D^{-1}] \tag{3.9}$$

Unfortunately, the above equation applies only where D^{-1} exists. As D for a matrix of strictly proper transfer functions is zero, the equation is not appropriate for obtaining Q_i by first determining P_i^{-1}.

Because of the unavailability of a direct solution using state space realizations, a solution method based on determining the ratio of the adjoint of P_i to $det(P_i)$ is attempted (17:231-233). The method is applied to determine each Q_i as the product of P_i^{-1} and P_e. The necessary polynomial product manipulations are carried out on MATRIX_x. Results of the manipulations yield what appeared to be acceptable inverses.

The Q_i thus determined are then tested. Results indicate that the Q_i do not result in MP $[P_iQ_i]^{-1}$. The inherent difficulty seems to lie in numerical inaccuracies. While some of the inaccuracies are attributable to having to round off elements of the q_{ij}, other inaccuracies are determined to be related to conversions between state space and transfer functions of the realizations in MATRIX$_x$.

For example, using the "eig" command, the eigenvalues of the A matrix given in this chapter are determined to be the values indicated in column 1 of the following table. Obtaining first the transfer function form of the state space realization, and then obtaining the roots of the denominator polynomial (the characteristic function), the roots are as indicated in column 2. Hence, even prior to manipulating the polynomials to form the adjoint and determinant needed to obtain the P_i^{-1}, a noticeable error is present. The size of the error is significant in that its size is the same as the accuracy of the linearized plant model. It is believed that the primary reason for the failure of this method lies in such numerical precision problems.

Table 3.2. Characteristic Eigenvalues of P

Eigenvalues of A	Roots of characteristic
-0.0272 - j0.0000	-0.0272 + j0.0000
-2.6973 + j0.0000	-2.6973 - j0.0000
-0.3908 - j2.9614	-0.3908 + j2.9614
-0.3908 + j2.9614	-0.3908 - j2.9614
-20.0000 + j0.0000	-19.9998 - j0.0000
-20.0000 + j0.0000	-20 0001 + j0.0001
-20.0000 + j0.0000	-20.0001 - j0.0001

The extent of the impact of the inaccuracies is provided in the following table. All three columns of the table are roots of the numerator polynomial of q_{111} whose largest term is of the order 1×10^{14}. Column entries have been rounded to four

significant digits. Column 1 are roots determined when numerical precision is kept at 16 significant digits. Column 2 are roots achieved when all numerators terms with magnitude less than 1×10^{-6} are rounded to zero at several steps in the computation process. Column 3 are roots achieved when all numerator terms with magnitude less than 1×10^{-3} are rounded to zero. The wide variability in numerator roots determined by using this second method make the appropriateness of the method questionable in this case.

The third method attempted is to solve for the Q_i directly by forming an equation of the form $Ax = 0$ and then determining the solution space of x. This is the method used in (12) to determine the Q_i matrices. To accomplish this an A matrix having more rows than columns is needed so that x is known to lie in the nullspace of A (17:68). To this end, the q_{ij} elements of Q_i are defined as polynomials of the form

$$q_{ij} = \frac{a_n s^n + a_{n-1} s^{n-1} + \ldots a_o}{b_w s^w + b_{w-1} s^{w-1} + \ldots b_o} \tag{3.10}$$

under the assumption that the a_i and b_i are real constants. Both sides of the above equation are next multiplied by the denominator polynomial. The resultant left hand term is then substracted from both sides to yield

$$[a_n s^n + a_{n-1} s^{n-1} + \ldots a_o] - q_{ij}[b_w s^w + b_{w-1} s^{w-1} + \ldots b_o] = 0 \tag{3.11}$$

Evaluating the above equality at a minimum of $n + w + 2$ frequencies, $q \geq n + w + 2$, the resultant set of linear equations is written in matrix form as follows.

Table 3.3. Factors of $q_{1_{11}}$

No Roundoff Made	10^{-6} Roundoff	10^{-3} Roundoff
0	0	0
+6.154D-9, -2.697	+53.89, -2.697	+84.93, -2.697
-144.7, -.2901	-9.431, -.2901	-8.965, -.2901
-.02719, -25.01	-.02719, -2.475	-.02719, -2.475
-5.072, +4.642		
-.3908 + j2.961	-.3908 + j2.961	-.3908 + j2.961
-.3908 - j2.961	-.3908 - j2.961	-.3908 - j2.961
-4.500 + j6.000	-4.499 + j6.000	-4.500 + j6.000
-4.500 - j6.000	-4.499 - j6.000	-4.500 - j6.000
-9.996 + j.07495	-10.67 + j1.371	-9.753 + j2.099
-9.996 - j.07495	-10.67 - j1.371	-9.753 - j2.099
-14.31 + j2.382	-12.59 + j5.381	-11.08 + j6.536
-14.31 - j2.382	-12.59 - j5.381	-11.08 - j6.536
-17.33 + j7.388	-14.29 + j11.72	-12.75 + j15.06
-17.33 - j7.388	-14.29 - j11.72	-12.75 - j15.06
-32.58 + j17.85	-32.92 + j.6940	-.2920 + j.3940
-32.58 - j17.85	-32.92 - j.6940	-.2920 - j.6940
+56.77 + j26.34	-13.69 + j43.52	-5.664 + j46.31
+56.77 - j263.4	-13.69 - j43.52	-5.664 - j46.31
+18.77 + j64.20	+20.74 + j43.52	
+18.77 - j64.20	+20.74 - j43.52	
-25.04 + j67.71		
-25.04 - j67.71		

$$\begin{pmatrix} 1\ j\omega_1\ (j\omega_1)^2 \ldots (j\omega_1)^n & \mathbf{q_{ij}(j\omega_1)}[1\ j\omega_1\ (j\omega_1)^2 \ldots (j\omega_1)^n] \\ 1\ j\omega_2\ (j\omega_2)^2 \ldots (j\omega_2)^n & \mathbf{q_{ij}(j\omega_2)}[1\ j\omega_2\ (j\omega_2)^2 \ldots (j\omega_2)^n] \\ \vdots & \vdots \\ 1\ j\omega_q\ (j\omega_q)^2 \ldots (j\omega_q)^n] & \mathbf{q_{ij}(j\omega_q)}[1\ j\omega_q\ (j\omega_q)^2 \ldots (j\omega_q)^n] \end{pmatrix} \begin{pmatrix} a_o \\ a_1 \\ \vdots \\ a_n \\ b_o \\ b_1 \\ \vdots \\ b_w \end{pmatrix}$$

To obtain the $\mathbf{q_{ij}(j\omega_i)}$ requires evaluating the product $\mathbf{P^+(j\omega)P_e(j\omega)}$ at frequency ω_i and extracting the ij element resulting from the evaluation.

To obtain a set of vectors spanning the nullspace of A, the modified Hermite normal form of A is obtained. The "rref" command in MATRIX$_x$ is used for this purpose. With the A matrix in Hermite noraml form, only those columns whose diagonal element is 0 span the nullspace of A. A " -1 " is inserted at the diagonal position to yield the spanning vector.

In using a routine based on this third method, only those spanning vectors whose coefficients are real can be used (i.e., the solutions must satisfy the assumption that the constants of equation 3.10 are real). Due to numerical imprecision, spanning vectors have typically been considered real if their imaginary components were on the order of 10^{-10} or less. However, in running the routine, imaginary components were always obtained with magnitudes well above the typical cut-off (on the order of 10^{-1} or 10^{-2}). As such, all solutions obtained by the above method were deemed unacceptable. The only explanation that is offered to explain failure of this algorithm is that the product $\mathbf{P^{-1}(j\omega)P_e(j\omega)}$ was ill-conditioned in the frequency region of interest.

A solution using a curve-fitting approximation to the $\mathbf{q_{ij}(j\omega_i)}$ points determined above was not attempted due to time considerations. Curve fitting approximations

would require not only iteratively fitting the curve, but also establishing the acceptability of successive approximations using the QFT criterion on the product $\mathbf{P}(j\omega)\mathbf{Q}(j\omega)$.

Finally, a solution based on determining the P_i^{-1} by first augmenting the numerator terms of transfer function elements of P_i with sufficient zeros at infinity (e.g., by multiplying each p_{ij} by $(s + 10^6)^2$) to make the D matrices of each P_i invertible so that Equation (3.9) can be applied was also not attempted due to time considerations.

IV. Conclusions and Recommendations

This thesis focused on the selection of a frequency sensitive weighting matrix $\mathbf{Q}(j\omega)$ to convert an original non-square $l \times m$ plant transfer matrix $\mathbf{P}(j\omega)$ into a square plant matrix appropriate for multiple-input, multiple-output (MIMO) quantitative feedback technique (QFT) design work. The plant was assumed to have more inputs than observable outputs. The method of pre-specifying an $l \times l$ desirable plant transfer matrix $\mathbf{P_e}(j\omega)$ for determining the necessary nonsquare, $m \times l$ weighting matrix $\mathbf{Q}(j\omega)$ was investigated.

While a number of conclusions concerning the selection of an optimal $\mathbf{Q}(j\omega)$ were established and summarized at the end of Chapter II, the basic problem of integrating QFT design criteria with norm-minimization criterion remains.

Difficulties encountered in obtaining Q_i indicate that it may be more advisable to pursue optimization methods that yield a $\mathbf{Q}(j\omega)$ directly. The processes followed in this study to obtain $Q_i = P_i^{-1} P_e$ did not provide suitable Q_i for the given plant and $\mathbf{P_e}(j\omega)$; numerical precision difficulties encountered in this study were sufficient to introduce RHP factors into $det(\mathbf{P_e}(j\omega))$ over the set of plant parameter variations even though $det(\mathbf{P}(j\omega))$ had no RHP factors over the set of all possible plant parameter variations.

The following recommendations for areas of future study are made:

1. Investigate the use of an H_2 or H_∞ optimal controller $\mathbf{Q}(j\omega)$ that robustly stabilizes all plants $\mathbf{P}(j\omega)$ in a set of possible plants $\mathcal{P}(j\omega)$ for the case where the disturbance $\mathbf{d_2}(j\omega)$ is zero.
2. Investigate the use of a Q_i whose numerator terms are the conjugates of some element $P_i \in \mathcal{P}_i$, the set of squared-down versions of that plant. Determine which $P_i \in \mathcal{P}_i$, if any, allow a cascaded $P_i Q_i$ pair to either reduce the band-

width over which diagonal dominance is not achieved or, if possible, satisfy Rosenbrock's diagonal dominance condition.

3. Continue the investigation effort of this study after identifying an acceptable method to obtain either the P_1^{-1} or the Q_i matrices. Determine if the use of the pre-specified $\mathbf{P_e}(j\omega)$ improves the effectiveness of a QFT design involving the given plant.

Bibliography

1. Adams, James M. *QFT Design of a Robust Landing Longitudinal Digital Controller for the AFTI/F16 Using MATRIXx*. MS thesis, Air Force Institute of Technology, Wright-Patterson AFB, Ohio 45433, March 1988.
2. Curtis, Charles W. *Linear Algebra* (third Edition). Boston: Allyn and Bacon, Inc., 1979.
3. D'Azzo, J.J. and C.H. Houpis. *Linear Control System Analysis and Design: Conventional and Modern* (third Edition). New York: McGraw-Hill Book Co., 1988.
4. Flight Dynamics Laboratory/AFWAL, Wright-Patterson AFB, OH 45433. *Flying Qualities of Piloted Vehicles, MIL-PRIME Standard and Handbook*, February 1986.
5. Francis, Bruce A. *A Course in H_∞ Control Theory*. Springer-Verlag, 1988.
6. Hamilton, Steven W. *QFT Digital Controller for an Unmanned Research Vechicle with an Improved Method for Choosing the Control Weightings*. MS thesis, Air Force Institute of Technology, Wright-Patterson AFB, Ohio 45433, December 1987.
7. Houpis, C. H. *Quantitative Feedback Theory (QFT) Technique for Designing Multivariable Control Systems*. Technical Report AFWAL-TR-86-3107, Wright-Patterson AFB, Ohio 45433: Flight Dynamics Laboratory/AFWAL, January 1987.
8. Integrated Systems, Inc., Palo Alto, California. *$MATRIX_x$ User's Manual*, 1988.
9. Isaac M. Horowitz, et al. *Research in Advanced Flight Control Design*. Technical Report AFFDL-TR-79-3120, Wright Patterson AFB, OH 45433: Flight Dynamics Laboratory/AFWAL, January 1980.
10. Kassan, Mark W. *F-16 Simulator for Man-in-the-Loop Testing of Aircraft Control Systems (SIMTACS)*. MS thesis, Air Force Institute of Technology, Wright-Patterson Air Force Base, Ohio 45433, December 1987.
11. Maybeck, Peter S. *Stochastic Models, Estimation, and Control*, Volume 1. New York: Academic Press, Inc., 1979.
12. Phillips, William D. *Selection of a Frequency Sensitive QFT Weighting Matrix Using The Method of Specified Outputs*. MS thesis, Air Force Institute of Technology, Wright-Patterson Air Force Base, Ohio 45433, December 1988.
13. Porter, B. and A. Manganas. *Self-Designing Digital Control Systems*. Final Report on Grant AFOSR-85-0208 USAME/DC/802/88, Salford, England: University of Salford, May 1988.

14. Qing-Guo Wang, Chun-Hui Zhou and You-Xian Sun. "Stability of Polynomial Matrices," *International Journal of Control*, *32* (1987).

15. Ridgely, D. Brett and Banda Siva S. *Introduction to Robust Multivariable Control*. Technical Report AFWAL-TR-85-3102, Wright-Patterson AFB, OH 45433: Flight Dynamics Laboratory/AFWAL, February 1986.

16. Schneider, Dean L. *QFT Digital Flight Control Design as Applied to the AFTI/F16*. MS thesis, Air Force Institute of Technology, Wright-Patterson AFB, Ohio 45433, December 1986.

17. Strang, Gilbert. *Linear Algebra and Its Applications* (third Edition). San Diego: Harcourt Brace Jovanovich, Inc., 1988.

18. Stremler, Ferrel G. *Introduction to Communication Systems* (second Edition). Reading, MA: Addison-Wesley Publishing Company, 1980.

19. Symbolics, Inc , Cambridge, Massachusetts. *VAX UNIX MACSYMA Reference Manual*, 1988.

20. Vidyasagar. "On Undershoot and Nonminimum Phase Zeros," *International Journal of Control*, *31* (1986).

21. Yaniv, O. "Quantitative Design Method for MIMO Uncertain Plants to Achieve Prescribed Diagonal Dominant Closed-Loop Minimum-Phase Tolerances," *International Journal of Control*, *47*:519–528 (1988).

22. Yaniv, O. and I. M. Horowitz. "A Quantitative Design Method for MIMO Linear Feedback Systems Having Uncertain Plants," *International Journal of Control*, *43*:401–421 (1986).

Vita

Captain George R. Rivard [redacted] In 1967, he [redacted] entered military service. In 1983, he received a Bachelor of Science Degree in Mathematics from the University of Alaska, Anchorage, Alaska, and was subsequently accepted to attend the USAF Officer Candidate School. Following his commission in the USAF in December that same year, he attended Auburn University, Auburn, Alabama and received a Bachelor of Science Degree in Electrical Engineering in 1985. He was assigned to Hanscom AFB, Bedford, Massachusetts as project engineer and alternate program manager for the Ultra Low Sidelobe Antenna (ULSA) Program Office from 1985 to 1988; ULSA was a multi-million dollar modification kit designed to improve performance of USAF AN/TPS-43E Radar Systems. During his assignment at Hanscon AFB, he received a Master of Science Degree in Engineering Management from Western New England College, Boston, Massachusetts, and completed certification as both an American Society for Qualilty Control Certified Quality Technician and Reliability Engineer, and as a Certified Professional Managers with the Institute of Professional Managers. In May 1988, he entered the School of Engineering, Air Force Institute of Technology.

REPORT DOCUMENTATION PAGE

Form Approved
OMB No. 0704-0188

1a. REPORT SECURITY CLASSIFICATION UNCLASSIFIED	1b. RESTRICTIVE MARKINGS
2a. SECURITY CLASSIFICATION AUTHORITY	3. DISTRIBUTION/AVAILABILITY OF REPORT Approved for public release; distribution unlimited.
2b. DECLASSIFICATION/DOWNGRADING SCHEDULE	
4. PERFORMING ORGANIZATION REPORT NUMBER(S) AFIT/GE/ENG/89D-43	5. MONITORING ORGANIZATION REPORT NUMBER(S)
6a. NAME OF PERFORMING ORGANIZATION School of Engineering 6b. OFFICE SYMBOL (If applicable) AFIT/ENG	7a. NAME OF MONITORING ORGANIZATION
6c. ADDRESS (City, State, and ZIP Code) Air Force Institute of Technology Wright-Patterson AFB, Ohio 45433	7b. ADDRESS (City, State, and ZIP Code)
8a. NAME OF FUNDING/SPONSORING ORGANIZATION AFIT/ENG 8b. OFFICE SYMBOL (If applicable)	9. PROCUREMENT INSTRUMENT IDENTIFICATION NUMBER
8c. ADDRESS (City, State, and ZIP Code) Air Force Institute of Technology Wright-Patterson AFB, Ohio 45433	10. SOURCE OF FUNDING NUMBERS PROGRAM ELEMENT NO. / PROJECT NO / TASK NO / WORK UNIT ACCESSION NO.
11. TITLE (Include Security Classification) Weighting Matrix Selection for QFT Designs	
12. PERSONAL AUTHOR(S) George R. Rivard, Capt, USAF	
13a. TYPE OF REPORT MS Thesis 13b. TIME COVERED FROM _____ TO _____ 14. DATE OF REPORT (Year, Month, Day) 1989 December 15. PAGE COUNT 105	
16. SUPPLEMENTARY NOTATION	

17. COSATI CODES			18. SUBJECT TERMS (Continue on reverse if necessary and identify by block number)
FIELD	GROUP	SUB-GROUP	
01	04		Quantitative Feedback Technique (QFT), H-2 norm Minimization, H-infinity norm Minimization, Flight Control

19. ABSTRACT (Continue on reverse if necessary and identify by block number)

Thesis Chairman: Zdzislaw H. Lewantowicz, Lt Colonel, USAF

20. DISTRIBUTION/AVAILABILITY OF ABSTRACT ☒ UNCLASSIFIED/UNLIMITED ☐ SAME AS RPT. ☐ DTIC USERS	21. ABSTRACT SECURITY CLASSIFICATION UNCLASSIFIED
22a. NAME OF RESPONSIBLE INDIVIDUAL Zdzislaw H. Lewantowicz, Lt Col, USAF	22b. TELEPHONE (Include Area Code) (513) 255-6913 22c. OFFICE SYMBOL AFIT/ENG

This thesis investigates the selection of the frequency sensitive weighting matrix needed to convert a nonsquare 1 x m plant matrix into a square plant matrix that satisfies Quantitative Feedback Technique (QFT) multiple-input, multiple-output design constraints. The method of pre-specifying a desirable plant matrix is used in determining the necessary weighting matrix. This study assumes that the nonsquare plant matrix has more inputs than outputs and the option to square-up is not available (i.e., it is assumed that inaccessible states cannot be reconstructed due to design limitations). Several topics are examined. The topics include energy and power spectral densities, singular value decompositions of matrices of transfer functions, QFT design constraints, QFT designs accomplished on nonsquare plants by breaking up the nonsquare plant into a sum of square plants, and both H-2 and H-infinity norm minimization. This study concludes with an examination of problems encountered in obtaining needed frequency sensitive weighting matrices and recommendations for areas of future study to avoid the described problems.